Pre-cachectic changes in amino acid homeostasis precede activation of eIF2α signaling in the liver at the onset of C26 cancer-induced cachexia

Ghita Chaouki, Laurent Parry, Cyrielle Vituret, Céline Jousse, Martin Leremboure, Céline Bourgne, Laurent Mosoni, Yoann Delorme, Mehdi Djelloul-Mazouz, Julien Hermet, et al.

iScience

Article

Pre-cachectic changes in amino acid homeostasis precede activation of eIF2α signaling in the liver at the onset of C26 cancer-induced cachexia

Graphical abstract

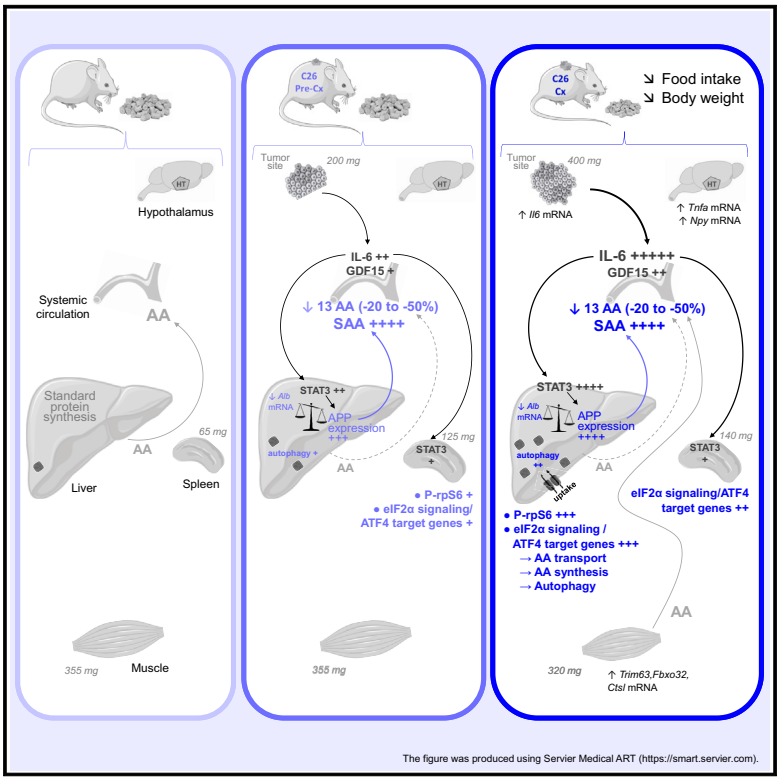

Highlights

- The production of positive APPs at the pre-Cx stage was as high as at the Cx stage
- Circulating levels of most amino acids were reduced as early as the pre-Cx stage
- EIF2α and rpS6 signalings were concomitantly activated in the liver at the onset of Cx
- ATF4 target genes promoting amino acid availability were overexpressed in Cx liver

Authors

Ghita Chaouki, Laurent Parry, Cyrielle Vituret, ..., Laure B. Bindels, Pierre Fafournoux, Anne-Catherine Maurin

Correspondence

anne-catherine.maurin@inrae.fr

In brief

Molecular biology; Cell biology; Cancer

Chaouki et al., 2025, iScience *28*, 112030
March 21, 2025
https://doi.org/10.1016/j.isci.2025.112030

CellPress

iScience

CellPress
OPEN ACCESS

Article

Pre-cachectic changes in amino acid homeostasis precede activation of eIF2α signaling in the liver at the onset of C26 cancer-induced cachexia

Ghita Chaouki,[1] Laurent Parry,[1] Cyrielle Vituret,[1] Céline Jousse,[1] Martin Leremboure,[2] Céline Bourgne,[3] Laurent Mosoni,[1] Yoann Delorme,[1] Mehdi Djelloul-Mazouz,[1] Julien Hermet,[1] Julien Averous,[1] Alain Bruhat,[1] Lydie Combaret,[1] Daniel Taillandier,[1] Isabelle Papet,[1] Laure B. Bindels,[4,5] Pierre Fafournoux,[1] and Anne-Catherine Maurin[1,6,*]

[1]Unité de Nutrition Humaine, INRAE, Université Clermont Auvergne, UMR 1019, F-63000 Clermont-Ferrand, France

[2]Université Clermont Auvergne, Clermont Auvergne INP, CNRS, Institut de Chimie de Clermont-Ferrand (ICCF), 63000 Clermont-Ferrand, France

[3]Digital PCR Platform Facility of the CHU of Clermont-Ferrand, 63000 Clermont-Ferrand, France

[4]Metabolism and Nutrition Research Group, Louvain Drug Research Institute, Université catholique de Louvain, UCLouvain, Brussels, Belgium

[5]Welbio Department, WEL Research Institute, Wavre, Belgium

[6]Lead contact

*Correspondence: anne-catherine.maurin@inrae.fr

https://doi.org/10.1016/j.isci.2025.112030

SUMMARY

The sequence of events associated with cancer cachexia induction needs to be further characterized. Using the C26 mouse model, we found that prior to cachexia, cancer progression was associated with increased levels of IL-6 and growth differentiation factor 15 (GDF15), highly induced production of positive acute phase proteins (APPs) and reduced levels of most amino acids in the systemic circulation, while signal transducer and activator of transcription 3 (STAT3) signaling was induced (1) in the growing spleen, alongside activation of ribosomal protein S6 (rpS6) and alpha subunit of eukaryotic translation initiation factor-2 (eIF2α) signalings, and (2) in the liver, alongside increased positive-APP expression, decreased *albumin* expression, and upregulation of autophagy. At the onset of cachexia, rpS6 and eIF2α signalings were concomitantly activated in the liver, with increased expression of activating transcription factor 4 (ATF4) target genes involved in amino acid synthesis and transport, as well as autophagy. Data show that pre-cachectic (pre-Cx) alterations in protein/aa homeostasis are followed by activation of eIF2α signaling in the liver, an adaptive mechanism likely regulating protein/amino acid metabolism upon progression to cachexia.

INTRODUCTION

A large proportion of cancer patients suffer from cachexia, a systemic wasting syndrome accelerating the deterioration of health. Cancer cachexia is characterized by a marked involuntary weight loss resulting from a combination of anorexia and atrophy of adipose and skeletal muscle tissues.[1–4] This represents one of the most detrimental side effects of cancer as advancing cachexia leads to functional impairments and a general weakness state that reduces tolerance and response to anticancer treatments. This syndrome can be considered as an immunometabolic imbalance resulting from neoplastic aggression. Indeed, the increased need of energy and building substrates due to tumor growth and activation of the immune system rapidly leads to systemic inflammation and major metabolic changes.[4–6] Despite these needs, marked anorexia most often appears during the pre-cachectic (pre-Cx) phase or in the early stages of cachexia, contributing significantly to body weight loss and the cachexia syndrome.[3,5]

Previous studies have characterized cancer cachexia as an increasingly perturbed state associated with inflammatory, metabolic and hormonal changes leading to alterations in behavior and body composition.[5] Progression to the cachectic (Cx) state involves both reciprocal effects between the tumor and host tissues and interactions between several tissues and organs (liver, adipose tissue, muscle, etc.).[5,7–9] Studies have highlighted the central role of some pro-inflammatory and stress cytokines in metabolic and food intake alterations during cachexia. These include tumor necrosis factor-α (TNF-α), interleukin (IL)-6, IL-1β, and growth differentiation factor 15 (GDF15),[8,10–14] whose release is progressively increased from the tumor site as the tumor grows. Particularly, IL-6 and GDF15 have been functionally involved in animal models of cancer anorexia-cachexia.[15–22] Nevertheless, the factors and events associated with the pre-Cx phase (before any weight loss) and transition to cachexia need to be better characterized.

During disease, the activity of many cell types is altered by a state of stress that may arise from the presence of foreign

components, the influx of stress mediators such as cytokines, or energy and nutrient deprivation. One of the mechanisms enabling the cell to cope with stress is the Integrated Stress Response, controlled by the phosphorylation of the alpha subunit of eukaryotic translation initiation factor-2 (eIF2α). eIF2α phosphorylation triggers both a reduction in protein synthesis in order to save resources and an adaptive gene expression program at the transcriptional level, through upregulated expression of activating transcription factor 4 (ATF4).[23–26] ATF4 notably regulates the expression of many genes involved in amino acid metabolism and responses to mitochondrial- and endoplasmic reticulum stresses.[24–30] Among the four kinases able to phosphorylate eIF2α in response to different kinds of stress, the general control non-derepressible 2 (GCN2) kinase (also known as Eif2ak4) is specifically activated by amino acid scarcities. Previous studies have highlighted the central role of the GCN2-eIF2α-ATF4 pathway in early food intake reduction response to nutritional stresses of one essential amino acid deficiency in the meal.[31–34] Furthermore, this signaling pathway has also been involved in upregulation of autophagy during amino acid deprivation in different cell types.[29,35–37]

In this study, our aim was to characterize early events resulting from tumor growth and preceding and/or being associated with the onset of the cachexia syndrome. For that purpose, we used the colon-26 adenocarcinoma (C26) mouse model of cancer cachexia[38] in which anorexia has been described as preceding or being concomitant with body weight loss,[19,39] as in humans.[3,5] At the pre-Cx stage, we found that the relatively moderate increase in IL-6 was associated with activation of signal transducer and activator of transcription 3 (STAT3) signaling in the spleen and liver, while in the systemic circulation, positive acute phase proteins (APPs) (serum amyloid A [SAA]) production was already very high and levels of most amino acids were markedly reduced. Furthermore, the data showed simultaneous activation of ribosomal protein S6 (rpS6) and eIF2α signalings and increased expression of ATF4 target genes involved in amino acid supply (1) in the spleen as early as the pre-Cx stage, and (2) in the liver at the onset of cachexia, suggesting upregulation of protein/amino acid metabolism in these organs early during cancer progression.

RESULTS

Characterization of the pre-Cx and Cx stages

A preliminary experiment enabled us to determine the kinetics of variation in food intake and body weight after C26 cell implantation (day 0), and to specifically define day 6 and day 8 post-implantation as corresponding to pre-Cx and early Cx stages, respectively (data not shown). We then carried out a second experiment to collect samples and analyze biological parameters from C26 mice at the pre-Cx or Cx stage, as well as from sham-injected mice. Food intake and body weight were measured daily from the day of implantation of C26 cells. On the 8th day, we observed a significant reduction in food intake of C26 mice compared to sham-injected mice (Figure 1A), associated with a decreased body weight (Figure 1B). At the pre-Cx stage, tumor weight was still modest (0.24 g or less than 1% of body weight) and it was increased by 1.7-fold at the Cx stage (Figure 1C). Spleen weight in pre-Cx mice was almost twice that of sham-injected mice, and did not increase further in the Cx group, while liver weight was similar in all groups. Heart weight was lower in the C26-Cx group than in the sham-injected group (Figure 1C). The weight of skeletal muscle, as assessed for the gastrocnemius plus soleus plus plantaris set, was found to not differ between the three groups following ANOVA; however, direct pairwise comparison between C26-Cx mice and sham-injected mice revealed reduced muscle weight in the C26-Cx group (around −10%; #p = 0.038, t test) (Figure 1C). Moreover, mRNA analyses in skeletal muscle confirmed an increased expression of the protein breakdown-related genes[40–43] *Trim63* and *Fbxo32* (encoding ubiquitin-protein ligases also known as MuRF1 and MAFbx, respectively), and *Ctsl* (encoding the cysteine protease cathepsin L) in the C26-Cx group, but not in the C26-pre-Cx group (Figure 1D). Thus, unlike the pre-Cx group, the Cx group was characterized by reduced food intake, body weight, and muscle mass, as well as increased expression of atrophy-related genes in skeletal muscle.

To further characterize early events linked to the onset of anorexia-cachexia, we analyzed the expression of neuropeptides involved in food intake control in the hypothalamus. We found that expression level of *Pomc*, encoding the anorectic neuropeptide pro-opiomelanocortin-alpha was unaltered, as measured at whole hypothalamus level, regardless of the group (see Figure S1A). By contrast, mRNA level of *Npy*, encoding the orexigenic neuropeptide Y, was 2-fold higher in the Cx group compared to sham-injected- and pre-Cx groups. This result supports previous data obtained with several animal models of cancer cachexia.[44–49] This could reflect an attempt of the organism to increase nutrient supply by using physiological mechanisms promoting food intake. In addition, we observed that mRNA level of the pro-inflammatory cytokine TNF-α was doubled in the hypothalamus of Cx mice compared to sham-injected- and pre-Cx mice, while mRNA levels of IL-1β and IL-6 remained unchanged (see Figure S1B). Thus, the onset of anorexia-cachexia was associated with an increased hypothalamic expression of *Tnfa* and *Npy*. However, we did not detect any variation of expression of these mRNAs in the hypothalamus of C26 pre-Cx mice compared to sham-injected animals (see Figure S1).

Increased production of IL-6 and GDF15 and reduced levels of most amino acids in systemic circulation as early as the pre-Cx stage

Both IL-6 and GDF15 have been functionally involved in cancer anorexia-cachexia.[15–22] Consistently, high plasma levels of both cytokines have been associated with cachexia in the C26 model.[18–20,50,51] We therefore measured circulating levels of these previously characterized critical factors to help contextualize our model in the progression from the pre-Cx to Cx stage. While IL-6 was almost undetectable in the sham-injected group, its mean concentration was 289 pg/mL in pre-Cx mice and reached 2,469 pg/mL in Cx mice (Figure 2A). As IL-6 concentration values followed a lognormal distribution, we performed a logarithmic transformation, which significantly increased the probability of a normal Gaussian distribution and highlighted that IL-6 concentration log-transformed values were significantly increased in pre-Cx- vs. sham-injected mice and further

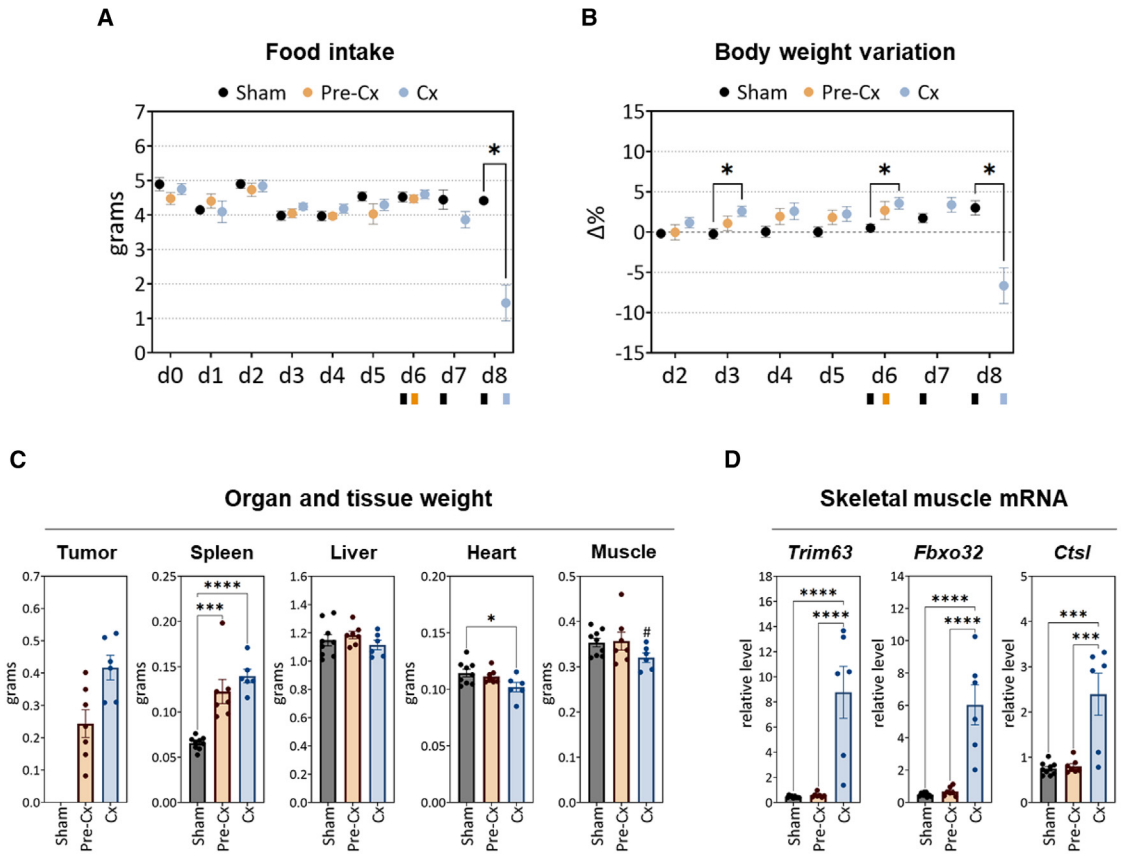

Figure 1. Unlike pre-Cx mice, Cx mice were characterized by reduced food intake, body weight, and muscle mass, as well as increased markers of skeletal muscle atrophy

At day 0, mice received either an implantation of 10^6 C26 cells (C26 tumor-bearing mice) or an injection of NaCl (sham-injected mice). C26 mice were necropsied either at day 6 (pre-Cx group) or day 8 (Cx group) and organs and tissues were weighed and samples harvested. The sham-injected group combined control mice obtained on days 6, 7, and 8 post-injection. Data are represented as mean ± SEM.

(A) Kinetic analysis of food intake. Food intake was measured every 24 h from the time point of implantation of C26 cells (day 0).

(B) Kinetic analysis of body weight. Body weight was measured every 24 h and expressed as a delta-percentage of reference values as measured at day 0.

(C) Organ and tissue weights at the time of sacrifice. Boxes below the graphs in (A) and (B) represent the sacrifice time points according to the different groups. Regarding skeletal muscle, the average weight of the set of gastrocnemius plus plantaris plus soleus is shown.

(D) Relative mRNA levels of atrophy-related genes in skeletal muscle (as compared to *Ywhaz* mRNA level). To assess the significance of differences in food intake and body weight between groups over time, two-way analyses of variance (ANOVA) were performed for each of these parameters and completed by Tukey's multiple comparison tests to analyze differences between groups at each time point. The first ANOVA, focused on data obtained up to day 6 for the three groups (sham, pre-Cx, and Cx), highlighted an overall significant effect of time ($p < 0.0001$), but no difference between groups neither for food intake or body weight. The second ANOVA took into account the sham-injected- and Cx groups from day 0 to day 8. Daily food intake was found to vary significantly according both to the presence of the tumor ($p = 0.0151$) and time ($p < 0.0001$), with a significant interaction between the two parameters ($p < 0.0001$). Analysis of the overall body weight data highlighted a significant effect of time on this parameter ($p = 0.0082$) as well as a significant interaction between the presence of the tumor and time ($p < 0.0001$).

For other analyses (C and D), the significance of differences between groups was assessed by one-way ANOVA followed by Tukey's multiple comparisons. (*$p < 0.05$; ***$p < 0.001$; ****$p < 0.0001$). In (C), the significance of the difference between the muscle weights of the Cx- and sham-injected groups was also assessed by direct pairwise comparison (#$p < 0.05$, t test). See also Figure S1.

elevated in Cx- vs. pre-Cx mice (Figure 2A). We also found that circulating GDF15 levels were gradually increased from 49 pg/mL in the sham-injected group to 105 pg/mL and 214 pg/mL in the pre-Cx- and Cx groups, respectively (Figure 2B). Thus, despite increased plasma levels of IL-6 and GDF15 at the pre-Cx stage, food intake was unaffected. Consistently, analysis of the relationship between plasma concentration of these cytokines and extent of food intake inhibition revealed a segmental profile with two linear regression segments (Figure 2C). According to these models, anorexia was associated with GDF15 and IL-6 concentrations above at least 131 pg/mL and 450 pg/mL, respectively. We also observed that both GDF15 and log-transformed IL-6 concentration values positively and linearly correlated with tumor weight (Figure 2D). Furthermore, *Il-6* mRNA expression at the tumor site was increased 2-fold in Cx- compared to pre-Cx mice, while *Gdf15* mRNA level remained unchanged (Figure 2E). In addition, mRNA levels of both cytokines were unaffected in peripheral tissues such as liver and

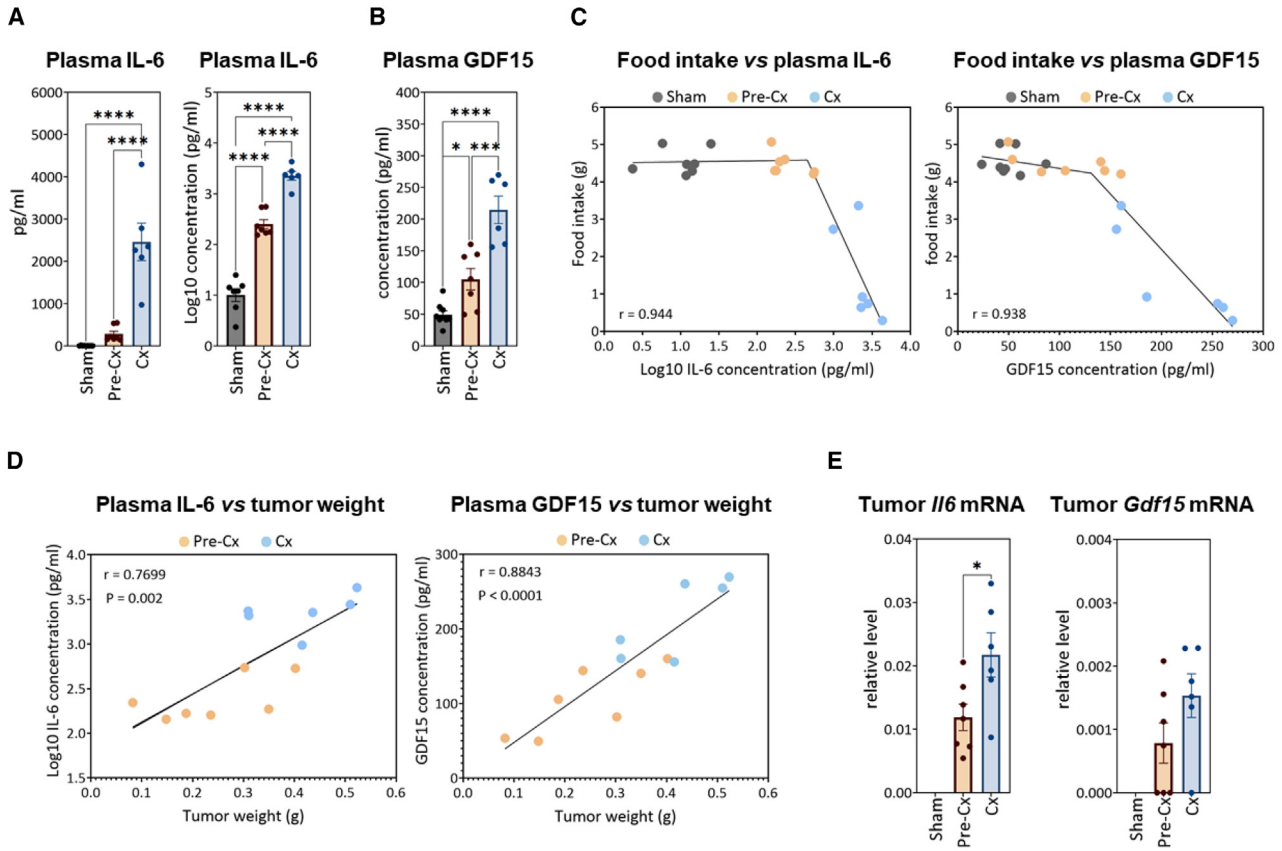

Figure 2. Comparative regulation of the cachectic cytokines IL-6 and GDF15 at pre-Cx and Cx stages

(A) Systemic circulating levels of IL-6 (real and log-transformed values).

(B) Systemic circulating levels of GDF15.

(C) Inverse relationship between plasma concentration of either IL-6 or GDF15 and food intake level. Data analysis using a non-linear regression test revealed a segmental linear relationship and a threshold effect (anorexia was associated with plasma GDF15 levels at least above 131 pg/mL and plasma IL-6 levels at least above log10 (2.653) pg/mL ≈ 450 pg/mL).

(D) Positive linear relationship between tumor weight and circulating IL-6 or GDF15 levels. The significance of the correlation between the two parameters was assessed by the Pearson's test.

(E) Relative mRNA levels of *Il-6* and *Gdf15* at the tumor site, as determined by digital qPCR (relative to *Ppia* mRNA level).

In (A), (B), and (E), data are represented as mean ± SEM. The significance of differences between groups in (A), (B), and (E) was assessed by one-way ANOVA followed by Tukey's multiple comparisons (*$p < 0.05$; ***$p < 0.001$; ****$p < 0.0001$). See also Figure S2.

intestine, at either the pre-Cx- or Cx stage (see Figure S2). Overall, these data show that tumor growth led to a significant increase in circulating levels of IL-6 and GDF15 before the onset of anorexia-cachexia, the latter being associated with plasma concentrations of these two cytokines above threshold values.

Next, since amino acid-homeostasis and -blood concentrations may be affected by neoplastic aggression, we measured amino acid levels in systemic circulation. Compared to sham-injected animals, C26 mice had reduced plasma concentrations of thirteen L-amino acids as early as the pre-Cx stage: tyrosine, threonine, asparagine, methionine, proline, serine, tryptophan, isoleucine, leucine, valine, lysine, histidine, and phenylalanine (Figure 3). For almost all these amino acids, this effect was also observed, with the same amplitude, in the Cx group. Interestingly, phenylalanine was the only amino acid whose level was higher at the Cx stage compared to the pre-Cx stage. The pre-Cx stage-related reduction concerned all essential amino acids, as well as some non-essential ones (Figure 3). The magnitude of the decrease ranged from 40% to 60% for tyrosine, threonine, asparagine, methionine, proline, and serine. Glycine tended to show the same profile, with a significant decrease at the Cx stage only (Figure 3). Cysteine was the only amino acid whose circulating level was higher in C26 mice than in sham-injected animals, and only at the pre-Cx stage. Finally, we did not observe any significant change in plasma concentration of glutamate, arginine, glutamine, and alanine. Overall, amino acid profiles in the systemic circulation were strongly affected at the pre-Cx stage, while food intake was unaffected.

During cachexia, it is recognized that the activation of muscle protein degradation aims to mobilize amino acids for transfer as substrates to the tumor and visceral organs.[6,52–54] Recourse to this deleterious process demonstrates the magnitude of the need, and suggests that reductions in circulating amino acid

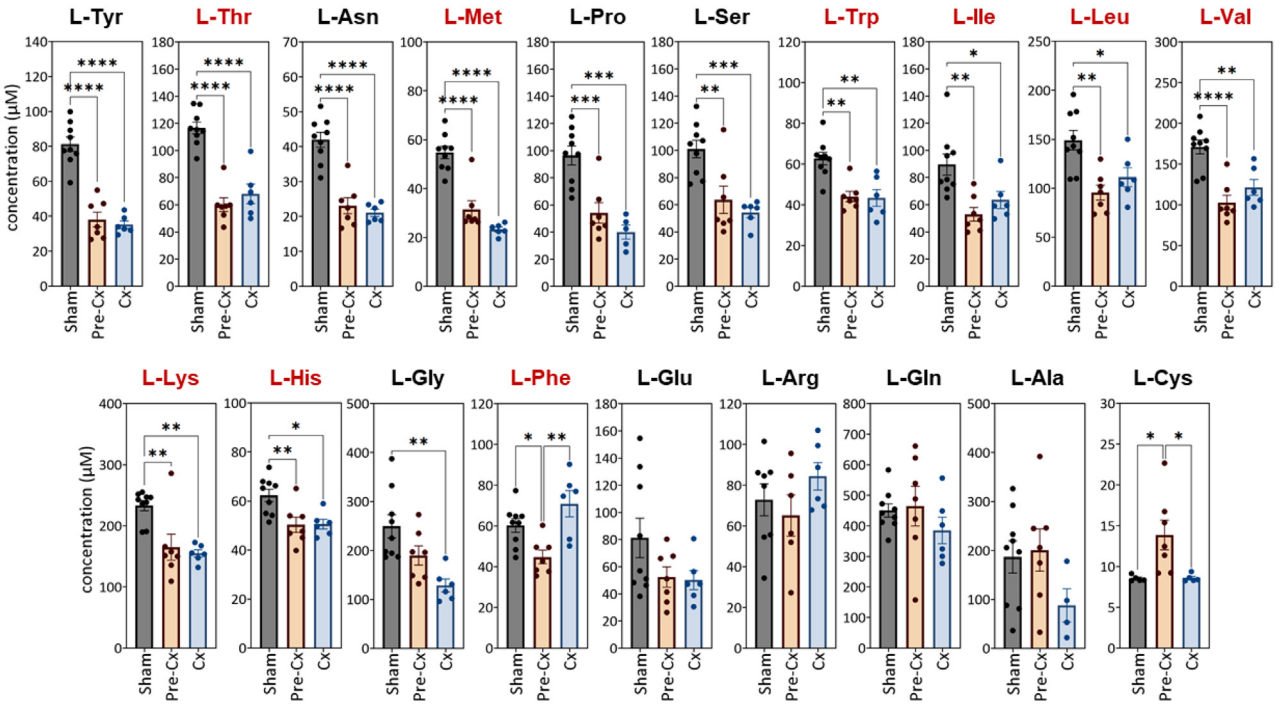

Figure 3. Marked reduction in the level of most amino acids in the systemic circulation as early as the pre-Cx stage

Blood was collected at the time of sacrifice by intra-cardiac puncture. Concentrations of the different amino acids were determined from plasma samples. Data are represented as mean ± SEM. The significance of differences between groups was assessed by one-way ANOVA followed by Tukey's multiple comparisons (*$p < 0.05$; **$p < 0.01$; ***$p < 0.001$; ****$p < 0.0001$). Essential amino acids are indicated in red.

levels as early as the pre-Cx stage may reflect an early increase in amino acid utilization at these sites.

Activation of signaling pathways regulating protein/amino acid homeostasis in the pre-Cx spleen

In C26 mice, spleen weight was increased by 2-fold as early as the pre-Cx stage (Figure 1C). This observation was consistent with data from literature indicating splenomegaly in C26 cancer-related cachexia.[18,55] As suggested elsewhere, this was likely to be the result of hyperfunction and immune hyperplasia, which could represent a significant consumption of amino acids.[56]

We first analyzed spleen responsiveness to inflammatory stimuli. Mechanistically, IL-6 has been shown to act mainly through activating STAT3.[56–60] We observed that (Tyr705)-STAT3 phosphorylation was induced in the spleen of C26 mice as early as the pre-Cx stage (Figure 4A), indicating activated state of this effector,[60,61] despite a rather moderate increase in circulating level of IL-6 at this stage (Figure 2A).

Then, we analyzed the activity of the two major signaling pathways involved in protein/amino acid homeostasis regulation, namely mechanistic target of rapamycin complex 1 (mTORC1)- and eIF2α-ATF4 signaling pathways, at the whole spleen level. mTORC1 kinase complex plays a key role in sensing amino acid availability and promoting protein synthesis accordingly, by notably activating rpS6 kinase (S6K1).[62] We examined the activity of S6K1, which reflects the impact of mTORC1 on protein synthesis, by analyzing the phosphorylation level of its substrate, rpS6. Interestingly, phosphorylation of (S240/244)-rpS6 was transiently upregulated in the spleen of C26 mice, at the pre-Cx stage only. The eIF2α-ATF4 signaling pathway is an important regulator of protein/amino acid homeostasis involved in cell adaptation to stress situations, by inhibiting translation and triggering an ATF4-mediated gene expression program including many genes involved in amino acid metabolism.[24–26,30,63] We observed that eIF2α signaling was activated in the spleen of C26 mice at both the pre-Cx and Cx stages, as evidenced by increased phosphorylation of eIF2α on Ser51 residue. Consistently, expression level of ATF4 target genes involved in amino acid synthesis (i.e., *Asns* and *Psat1*, involved in asparagine and serine synthesis, respectively) (Figure 4B) and amino acid transport (i.e., *Slc7a1* and *Slc7a5*, encoding CAT-1 and LAT1 plasma membrane amino acid transporters, respectively) (Figure 4C) was increased at the pre-Cx stage, an effect that was clearly enhanced at the Cx stage.

Thus, alongside increased spleen size at the pre-Cx stage, signaling pathways regulating amino acid availability and utilization were activated in this organ, probably to cope with elevated rates of protein and nucleotide synthesis linked to tumor-induced immune cell proliferation.

Strong induction of positive-APP production as early as the pre-Cx stage

In addition to supporting active cell proliferation in spleen and tumor, increased amino acid requirements may result from highly induced synthesis of exported proteins specifically involved in

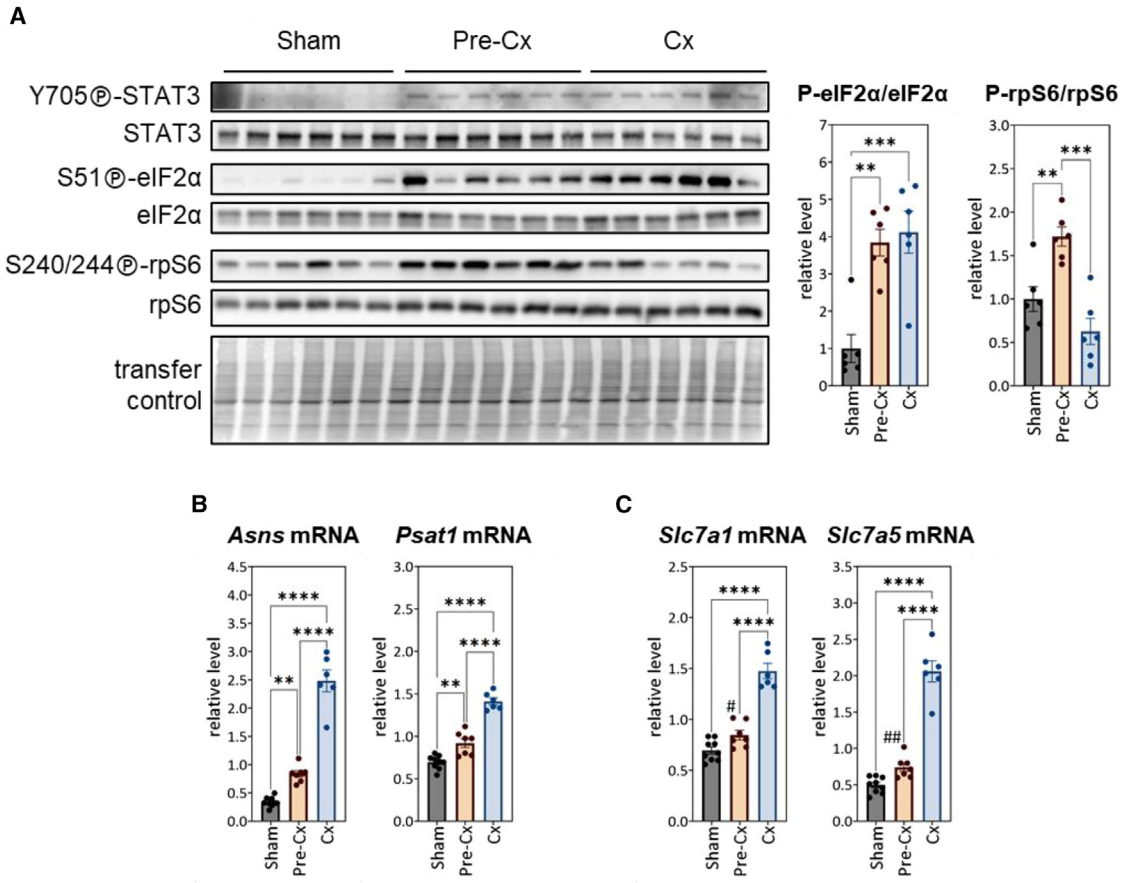

Figure 4. Activation of molecular pathways related to inflammatory cytokine signaling and regulation of protein/amino acid metabolism in the pre-Cxspleen

(A) Analysis of [Y705]-STAT3, (S51)-eIF2α and (S240/244)-rpS6 phosphorylation by western-blot. TGX signals were used to control protein transfer efficiency. For each mouse, the calculation of the ratio between the signal intensity of the phosphorylated form and the signal intensity of the total form was performed. The significance of differences between groups was assessed by one-way ANOVA followed by Tukey's multiple comparisons (**$p < 0.01$; ***$p < 0.001$). Data are represented as mean ± SEM.

(B and C) mRNA levels of ATF4-target genes involved in amino acid biosynthesis (B) and amino acid transport (C) expressed relative to *Ppia* mRNA level. The significance of differences between groups was assessed by one-way ANOVA followed by Tukey's multiple comparisons (**$p < 0.01$; ****$p < 0.0001$). In (C), the significance of differences between the relative mRNA levels in the pre-Cx- and sham-injected groups was also assessed by direct pairwise comparison (#$p = 0.018$ and ##$p = 0.002$ by t test). Data are represented as mean ± SEM.

response to acute inflammation. APPs are blood proteins highly produced as part of the acute phase response (APR), an early defense and protection system activated during various types of aggression.[64,65] Members of the SAA family, major positive APPs in mice and humans, are extensively produced during acute inflammation.[64,65] We found that SAA levels were dramatically increased in the systemic circulation in C26 mice as early as the pre-Cx stage (mean concentration 2.79 mg/mL), an effect that was not amplified at the Cx stage (mean concentration 2.82 mg/mL) (Figure 5A).

Hepatocytes are considered the main source of APPs.[66] In liver, we observed that expression of *Saa1*, *Saa2*, and *Apcs*, encoding three major positive APPs (two SAA isoforms and the serum amyloid P component, respectively) was strongly induced at the pre-Cx stage, and further increased at the Cx stage (Figure 5B). As IL-6 has been directly involved in upregulation of APP expression,[67–70] we plotted hepatic *Saa1* and *Saa2* mRNA levels as a function of circulating IL-6 concentration for each animal (i.e., data given in Figure 2A), an analysis that revealed a strong correlation between the two parameters (Figure 5C). Conversely, mRNA level of albumin, a negative APP, was decreased by 35% as early as the pre-Cx stage (Figure 5B). Mechanistically, IL-6 has been shown to regulate positive-APP gene expression mainly through activating STAT3 signaling,[56–59,71,72] and previous work has evidenced STAT3 signaling activation in the liver of Cx C26 mice.[73] Consistently, we observed that (Tyr705)-STAT3 phosphorylation was clearly induced in the liver of C26 mice as early as the pre-Cx stage, indicating activated state of this transcription factor (Figure 5D). Thus, even before the onset of cachexia, cancer progression elicited a huge induction of positive-APP production, while *albumin* expression was reduced.

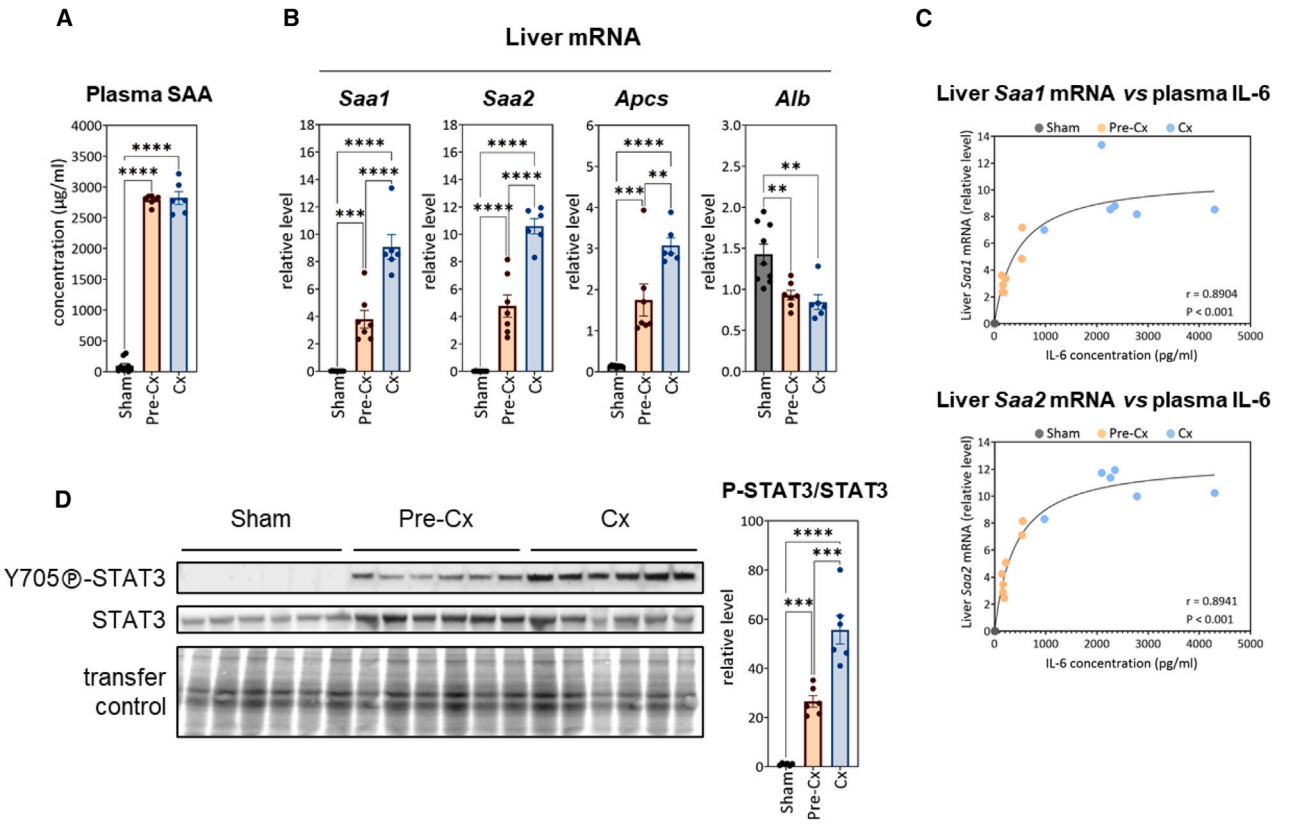

Figure 5. Huge induction of positive-APP production as early as the pre-Cx stage

(A) Systemic circulating levels of SAAs.

(B) Relative mRNA levels of *Saa1*, *Saa2*, *Apcs*, and *Alb* in the liver (as compared to *Ppia* mRNA level).

(C) Strong correlation between IL-6 circulating levels and SAA gene expression in the liver of C26 mice. A Spearman correlation test was performed.

(D) Western-blot analysis of (Tyr705)-STAT3 phosphorylation. For each mouse, the calculation of the ratio between the signal intensity of the phosphorylated form and the signal intensity of the total form was performed. TGX signals were used to control protein transfer efficiency.

In (A), (B), and (D), data are represented as mean ± SEM, and the significance of differences between groups was assessed by one-way ANOVA followed by Tukey's multiple comparisons (**$p < 0.01$; ***$p < 0.001$; ****$p < 0.0001$).

Upregulation of mechanisms promoting amino acid availability and utilization in the liver at the transition from the pre-Cx to Cx stage

The liver plays a central role in the regulation of protein/amino acid homeostasis, releasing many amino acids used by other organs and tissues,[74] and producing the majority of proteins exported to plasma.[75] We therefore carried out additional analyses to investigate parameters related to amino acid utilization and availability in the liver.

We first observed that (S240/244)-rpS6 phosphorylation was unaffected at the pre-Cx stage, but strongly increased in livers of Cx mice compared to sham-injected- and pre-Cx mice (Figure 6A), suggesting an increase in mTORC1/S6K1-mediated hepatic protein synthesis at the onset of cachexia. Then, as autophagy is a degradation process that can provide substantial amounts of amino acids through lysis of endogenous liver proteins,[76–78] we analyzed the lipidation of MAP1LC3B protein (microtubule-associated protein 1 light chain 3 beta, LC3B) as a major marker of autophagosome formation by western blotting. The signal ratio between the lipid-bound LC3B-II form and the cytosolic LC3B-I form increased at pre-Cx and Cx stages, indicating upregulation of autophagy (Figure 6B). mTORC1 regulates autophagy.[62] By notably phosphorylating the autophagy-initiating serine/threonine-protein kinase Unc-51-like kinase 1 (ULK1) on Ser757 residue, mTORC1 inhibits autophagy when amino acids are available.[79–82] Western blot analysis of liver protein extracts showed that intensity of the phospho-(Ser757)-ULK1 signal varied within groups (see Figure S3). However, the signal intensity ratio between the phosphorylated and total forms (phospho-(Ser757)-ULK1/ULK1) was lower in the pre-Cx group than in the sham-injected group. Moreover, this decrease was more an effect of increased total ULK1 signal (see Figure S3), a parameter that has already been considered as an indicator of upregulated autophagy in previous studies.[83,84] On the whole, these results support an upregulation of autophagy at the pre-Cx stage.

We then analyzed the eIF2α-ATF4 signaling pathway as a major regulator of protein/amino acid homeostasis.[24–26] In addition to inhibiting translation, eIF2α phosphorylation has been shown to trigger an ATF4-mediated gene expression program including

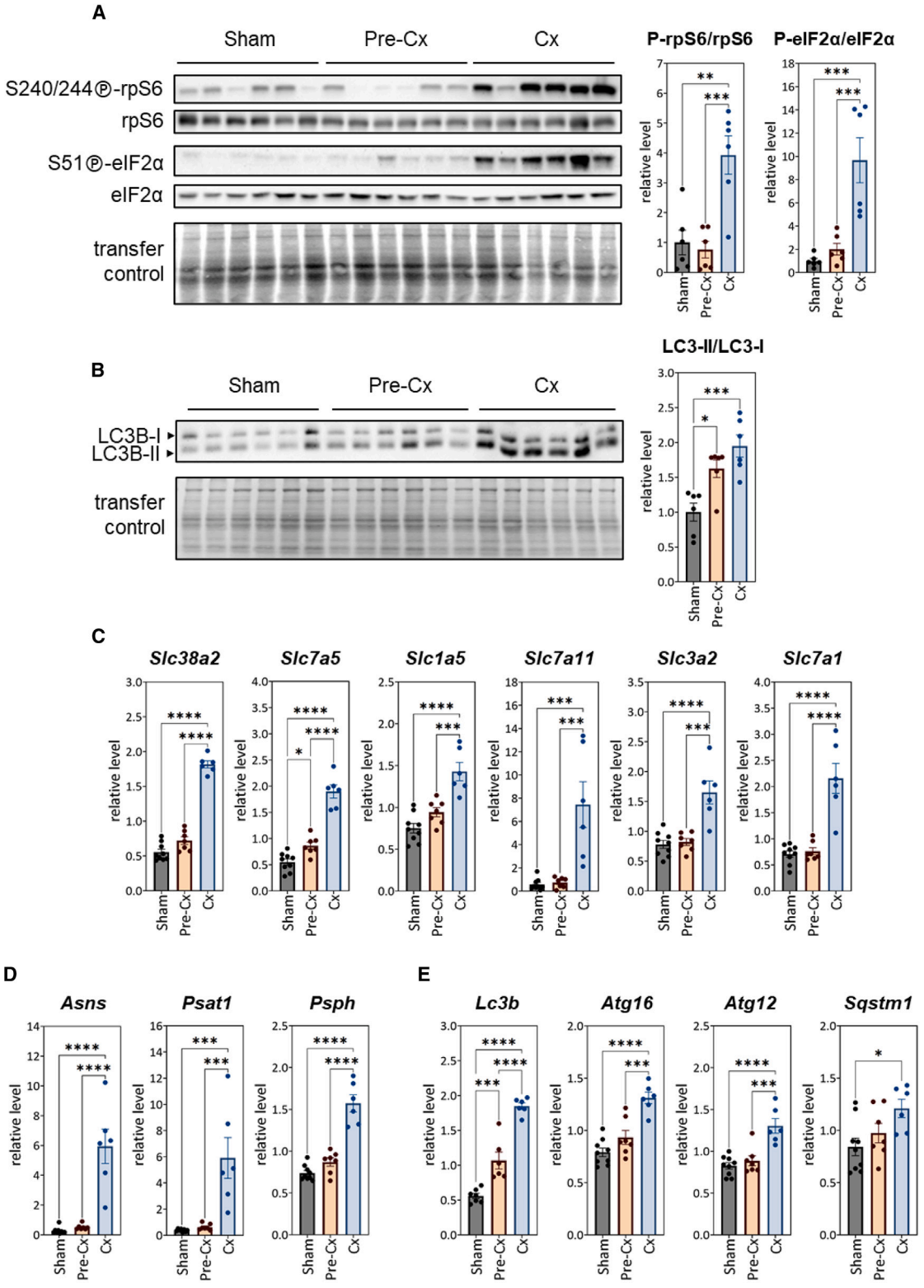

(legend on next page)

many genes involved in amino acid metabolism.[24–26,29,30,63] We found that eIF2α phosphorylation was not affected at the pre-Cx stage but was clearly induced in the liver of Cx mice (Figure 6A). Consistently, expression levels of the ATF4-target genes *Slc38a2*, *Slc7a5*, *Slc1a5*, *Slc7a11*, *Slc3a2*, and *Slc7a1*, encoding several plasma membrane amino acid transporters,[27,30,85–87] were markedly increased in the liver of C26-Cx mice compared to sham-injected and pre-Cx mice (Figure 6C). Moreover, mRNA levels of ATF4 target genes involved in amino acid synthesis[27,30,88] (i.e., *Asns*, *Psat1*, and *Psph*) (Figure 6D) and autophagy[29] (i.e., *Lc3b*, *Atg16l1*, *Atg12*, and *Sqstm1*) (Figure 6E) were also clearly upregulated in livers of C26-Cx mice. Interestingly, relative expression levels of *Asns* and *Psat1*, involved in asparagine and serine synthesis, were increased 22- and 15-fold, respectively, in livers of Cx mice compared to sham-injected animals (Figure 6D). These results suggest that ATF4 may contribute to promoting the availability of amino acids in the liver from the onset of cachexia, by upregulating the expression of genes involved in amino acid biosynthesis and amino acid transport, as well as autophagy, at a time when high phosphorylation of rpS6 likely indicates an mTORC1-mediated increase in liver protein synthesis.

DISCUSSION

In this study, we examined events associated with the pre-Cx stage and early cachexia during cancer progression, and related to protein/amino acid metabolism. We found that in systemic circulation, pre-Cx cancer progression was associated with moderate increases in IL-6 and GDF15 concentrations, dramatic induction of positive-APP production and marked reductions in the levels of most amino acids. STAT3 signaling was activated in the spleen and liver as early as the pre-Cx stage. This was associated with upregulated rpS6 and eIF2α signalings in the spleen, coinciding with an early and marked increase in the size of this organ. In the liver, an increase in the expression of positive-APPs, a decrease in the expression of albumin and an upregulation of autophagy occurred at the pre-Cx phase, while at the onset of cachexia, rpS6 phosphorylation and eIF2α signaling were strongly activated in this organ, along with increased expression of ATF4-target genes involved in amino acid synthesis and transport, as well as autophagy. Thus, neoplastic aggression had a strong impact on amino acid homeostasis even before the onset of cachexia, and progression to cachexia was associated with activation of adaptive mechanisms involved in regulating amino acid availability and utilization in the spleen and liver, including mTORC1 and eIF2α-ATF4 signaling pathways, presumably to cope with the sharp increase in (1) cell growth and (2) positive-APP production, respectively, in these organs.

We found elevated circulating levels of IL-6 and GDF15 at established cachexia, in agreement with previous studies using the C26 tumor-bearing mouse model,[18–20,51,89] but also moderately increased levels of these cytokines at the pre-Cx stage. These two cytokines have been functionally involved in cancer cachexia.[15–22] According to data from literature, GDF15 and IL-6 are likely produced at the tumor site,[4,15,90] composed of cancer cells as well as various infiltrated cell populations in the tumor microenvironment.[7,91] In line with this, we found that levels of *Il-6* mRNA were not affected in peripheral tissues (liver and intestine) of C26 mice, but were almost doubled at the tumor site in the Cx group compared to pre-Cx group. Since tumor weight almost doubled between these two stages, the combined effects of increased expression and increased tumor size could explain the exponential rise in circulating levels of IL-6. *Gdf15* mRNA levels were not altered in peripheral tissues or at the tumor site, even at an early stage of cachexia. Nevertheless, we can speculate that the nearly 2-fold increase in tumor size between the pre-Cx and Cx stages could have led to the observed linear increase in circulating levels of GDF15, even with a stable production rate at the tumor site, as well as to the strong linear correlation between circulating GDF15 levels and tumor weight ($r = 0.8843$). Importantly, increased circulating levels of IL-6 and GDF15 were observed even before any reduction in food intake, body weight, or muscle mass, and these levels were further elevated at the onset of anorexia-cachexia. Regarding GDF15 anorectic action, such a threshold effect has been suggested in other studies.[92–94] Since GDF15 has been shown to perform a number of diverse functions in addition to regulating food intake,[95] this cytokine was likely to be involved in aspects other than anorexia during pre-cachexia. Regarding IL-6, given that its STAT3-dependent effector signaling was activated at least in liver and spleen at the pre-Cx stage, we can assume that this cytokine induced/initiated, early and at relatively moderate levels, changes in target tissue functions, such as stimulation of hepatic positive-APP production.

We observed that a significant reduction (−25% to −60%) in systemic circulating levels of many amino acids was associated with tumor growth as early as the pre-Cx phase, demonstrating that reduced dietary intake was not involved. Consistently, in a study using the MAC16 transplant mouse model, which does not affect food intake, the authors observed that the Cx state

Figure 6. Upregulation of mechanisms promoting amino acid availability and utilization in the liver during the transition from pre-Cx to Cx stage

(A) Western-blot analysis of (S240/244)-rpS6 phosphorylation and (S51)-eIF2α phosphorylation. For each mouse, the ratio between the signal intensities obtained for the phosphorylated form and the total form, respectively, was calculated.

(B) Western-blot analysis of LC3B conversion. For each mouse, the ratio between the signal intensities obtained for the lipidated form anchored in the autophagosome membrane (LC3-II), and for the cytosolic form (LC3-I), respectively, was calculated. Increased ratio was an indicator of new autophagosomes recruitment.

In (A) and (B), TGX signals were used to control protein transfer efficiency.

(C–E) mRNA levels of ATF4-target genes involved in amino acid transport (C), amino acid biosynthesis (D), and autophagy (E), expressed relative to *Ppia* mRNA level. All data are represented as mean ± SEM. The significance of differences between groups was assessed by one-way ANOVA followed by Tukey's multiple comparisons (*$p < 0.05$; **$p < 0.01$; ***$p < 0.001$; ****$p < 0.0001$). See also Figure S3.

was associated with decreased plasma concentrations of most of the amino acids analyzed.[96] Furthermore, using the C26 mouse model, previous works have highlighted that cancer-related cachexia results in a unique metabolic imprint distinct from caloric restriction alone, including reduced levels of specific amino acids.[97,98] In line with a recent study,[99] our data support the idea that the decrease in levels of most amino acids in the systemic circulation is an early event that occurs during tumor growth prior to cachexia, and is not primarily related to a reduction in food intake and/or body weight. This could be the result of enhanced amino acid utilization to meet energy and nitrogen substrate requirements associated with increasing tumor and spleen size, as well as increased production of immune-related proteins. Indeed, over the course of cachexia, it is recognized that amino acids are mobilized from muscles and transferred to visceral organs and the tumor,[6,52–54] suggesting that amino acid requirements may be increased as early as during pre-Cx tumor progression. In the growing spleen, we observed that signaling pathways regulating utilization and availability of amino acids were activated as early as the pre-Cx stage, probably to cope with tumor-induced immune cell proliferation. Consistently, previous studies in rats have demonstrated increased protein synthesis in the spleen during acute inflammation.[100] However, although the activation of immune cell proliferation has an impact on amino acid requirements in inflammatory states, this demand has been estimated to be much lower than that associated with positive APP production by the liver.[101] Liver amino acid uptake and protein synthesis have been shown to be increased in cancer patients and in tumor-bearing rodent models during cachexia.[54,102–105] Given that, under normal conditions, the liver releases many amino acids that are consumed by the rest of the body, thereby regulating systemic amino acid availability,[74,75] it is likely that the strong enhancement of amino acid utilization by the liver itself, due to increased positive-APP synthesis and/or gluconeogenesis, may affect circulating amino acid levels as early as the pre-Cx stage. Over time, the maintenance of a state of protein/amino acid hypermetabolism must raise a challenge in terms of amino acid supply to meet needs. During cachexia, amino acid release from muscle proteolysis may be expected to restore circulating concentrations of some amino acids to normal/basal levels or even higher, as previously observed for phenylalanine in Cx C26 mice.[97,106] Consistently, we found that phenylalanine was the only amino acid with higher circulating levels at early cachexia compared to the pre-Cx state.

We found that pre-Cx reductions in systemic levels of amino acids, particularly all essential amino acids whose main fate is protein synthesis,[107] were associated with a strong induction of positive-APP production, suggesting increased amino acid utilization by the liver as the main source of these exported proteins. However, unaltered rpS6 phosphorylation in livers of pre-Cx mice suggested that mTORC1-S6K1 axis-related protein synthesis regulation was unaffected at this stage. Interestingly, hepatic expression and production of negative APPs, including albumin, were shown to be reduced in tumor-bearing or infected rodents.[51,97,108–110] While previous work has shown that *Alb* mRNA levels are reduced in Cx C26 mice,[97] in the present study we found that they were already significantly reduced at the pre-Cx stage. Mechanistically, the TNF-α-CCAAT enhancer binding protein beta (C/EBPβ) axis has been shown to be involved in reducing albumin gene transcription.[110–112] Given that albumin, the most abundant protein in plasma (around 35–40 mg/mL), accounts for 15% of hepatic protein synthesis[113] and has an expression that is mainly regulated at the transcriptional level,[112] this decrease in *Alb* mRNA levels probably allows a substantial saving of amino acids in the liver. Alternatively, increased hepatic autophagy could also have favored amino acid availability.

Persistent APR with continuous APP-positive production is likely to contribute to the etiology of cachexia.[114–116] It is therefore important to characterize the kinetic evolution of hepatic protein/amino acid metabolism regulation during tumor progression before and upon induction of the syndrome. Data from the present study demonstrated activation of eIF2α signaling, a major regulator of protein/amino acid metabolism, in the liver at the onset of cachexia. In response to various cellular stresses, eIF2α phosphorylation results in both rapid inhibition of translation and increased expression of ATF4 target genes.[24–26,30] At the whole organism level, this signaling pathway has been shown to play an important role in liver's adaptive response to dietary restriction of essential amino acids.[63,117,118] Our previous work has shown that the eIF2α-ATF4 signaling pathway is not activated by 24 h fasting.[119] In the present study, the activation of eIF2α signaling may have resulted from sensing reduced or imbalanced amino acid availability or endoplasmic reticulum (ER) or mitochondrial stress associated with disrupted liver tissue homeostasis, through one or more eIF2α kinases. Consistently, increased expression of unfolded protein response (UPR) markers has been previously reported in the liver of Cx C26 mice,[120] reinforcing the idea that adaptive mechanisms to cellular stress are triggered in this organ. These mechanisms may include adaptive upregulation of autophagy, to provide amino acids and/or remove damaged cellular components.[121,122] In this study, we found that autophagy was upregulated in the livers of C26 mice as early as the pre-Cx stage, an effect that was enhanced at the onset of cachexia, with upregulation of ATF4-target autophagy genes. These findings support those of a previous study showing increased autophagy markers in the livers of Cx C26 mice.[120] Given that eIF2α phosphorylation has been shown to promote autophagy, both through non-transcriptional effects and through ATF4-dependent activation of autophagy gene expression,[29,37,122] data from the present study suggest a contribution of the eIF2α-ATF4 signaling pathway to increased hepatic autophagy from the onset of cachexia. Furthermore, the phosphorylation of eIF2α is known as an effective inhibitor of translation; however, we observed a concomitant marked increase in rpS6 phosphorylation in the liver at the onset of cachexia, consistently with previous studies having demonstrated an overall increase in hepatic protein synthesis in Cx rodents.[54,102–105,123] On the other hand, cachexia was shown to be associated with a specific reduction in structural protein synthesis in the liver of colon cancer patients, concomitant with elevated hepatic production of positive APPs,[124] suggesting the implementation of differential regulations of protein synthesis. Interestingly, recent data showed that translation attenuation following eIF2α phosphorylation is not uniform across all coding transcripts, preferentially affecting mRNAs encoding long-lived proteins.[125] Such mechanisms could be involved in differential

regulation of translation upon stress, depending on the function of the proteins synthesized. Following eIF2α phosphorylation, upregulated ATF4 activates the expression of specific target genes involved in adaptation to stress, including many genes involved in protein/amino acid metabolism.[24–26,30] In our study, we show that expression of ATF4-regulated genes involved in amino acid transport, amino acid synthesis and autophagy was clearly increased at the onset of cachexia, suggesting a role of ATF4 in promoting amino acid availability in the liver. Interestingly, previous works have highlighted the possibility of a coordinated action between mTOR, as a kinase stimulating protein synthesis, and ATF4, as a transcription factor promoting amino acid availability, in anabolic settings in cultured mouse fibroblasts and *in vivo* in mouse liver.[126,127] One can speculate that the implementation of such coordination could contribute to maintaining a high level of positive-APP production in the liver over the course of cachexia. Further studies are needed to functionally explore and precisely determine the role of the eIF2α-ATF4 signaling pathway in the liver during cancer progression, upon induction and evolution of cachexia.

It is known that the pathophysiology of cancer cachexia involves imbalances in protein and energy metabolism, driven by inflammation. However, better characterization and precise kinetics of early metabolic changes associated with tumor growth and cachexia induction are needed. Data from the present study highlight early cancer-related alterations in protein/amino acid homeostasis and activation of mechanisms regulating protein/amino acid metabolism in spleen and liver during progression to cachexia, likely involving the eIF2α-ATF4 signaling pathway. Exploring the role of eIF2α signaling in the regulation of whole-body protein/amino acid homeostasis during cancer progression will require further investigations.

Limitations of the study

This study did not include measurements of overall hepatic protein synthesis. However, the data suggest that eIF2α phosphorylation-related attenuation of translation and mTOR/S6K1-dependent increase in protein synthesis may occur simultaneously in the liver at the onset of cachexia. This could indicate the implementation of differential regulations of synthesis of liver proteins according to their function. Thus, in parallel with measurements of overall protein synthesis, future studies should include characterization of such mechanisms and determining their role in regulating hepatic protein/amino acid metabolism during cancer progression, upon induction and evolution of cachexia.

Our data suggest an important role of the eIF2α-ATF4 signaling pathway as an adaptive regulatory mechanism of protein/amino acid metabolism in spleen and liver during the progression to cachexia. Functional studies will be required to assess the extent of its contribution, and should include analysis of amino acid import/export fluxes at the hepatic level.

As our study was carried out on male mice, the results cannot be generalized to females. Furthermore, we chose a mouse model of fairly acute cancer cachexia, with anorexia and body weight loss appearing rapidly after C26 cell implantation. Alterations in protein/amino acid homeostasis will need to be studied in other models, with detailed kinetic profile of parameters related to protein/amino acid metabolism before and at the onset of cachexia.

RESOURCE AVAILABILITY

Lead contact

Further information and requests for resources and reagents should be directed to and will be fulfilled by the lead contact, Anne-Catherine Maurin (anne-catherine.maurin@inrae.fr).

Materials availability

This study did not generate new unique reagents.

Data and code availability

- Data supporting the findings of this study are included within the article or its supplemental information.
- This article does not report original code.
- Any additional information required to reanalyze the data reported in this paper is available from the lead contact upon request.

ACKNOWLEDGMENTS

This work was supported by the Fondation pour la Recherche Médicale (FRM-labeled team, DEQ20180339180, France) and the Institut National de Recherche pour l'Agriculture, l'Alimentation et l'Environnement (INRAE, France). G.C. received financial support from the "Région Auvergne-Rhône-Alpes" (CPER EPICURE, Nex-N-Mob, France); we thank Dr. Didier Rémond (Unité de Nutrition Humaine, INRAE, Université Clermont Auvergne, France) for his help in this respect. We thank the staff of the Digital PCR Platform of the CHU of Clermont-Ferrand (France), our research unit's animal facility and the Mass Spectrometry Platform Facility of the Chemistry Institute of Clermont-Ferrand (France).

AUTHOR CONTRIBUTIONS

Conceptualization, G.C., P.F., and A.-C.M.; formal analysis, G.C., L.P., M.L., C.B., I.P., L.M., P.F., L.B.B., and A.-C.M.; funding acquisition, P.F., D.T., and A.-C.M.; investigation, G.C., L.P., M.L., C.B., Y.D., and M.D.-M.; methodology, L.B.B., C.V., G.C., D.T., and A.-C.M.; project administration, A.-C.M.; resources, L.B.B.; supervision, J.H., P.F., and A.-C.M.; visualization, L.B.B., I.P., L.M., and P.F.; writing – original draft, G.C., P.F., M.L., C.B., and A.-C.M.; writing – review & editing, L.B.B., C.J., I.P., L.M., D.T., A.B., J.A., and L.C. All authors approved the version to be published.

DECLARATION OF INTERESTS

The authors declare no competing interests.

STAR★METHODS

Detailed methods are provided in the online version of this paper and include the following:

- KEY RESOURCES TABLE
- EXPERIMENTAL MODEL AND STUDY PARTICIPANT DETAILS
  - Cell culture
  - Animal experiments
- METHOD DETAILS
  - RNA extraction & cDNA synthesis
  - Digital qPCR
  - Conventional qPCR
  - Protein extraction
  - Western-blot analysis
  - Antibodies
  - ELISA
  - Plasma amino acid analysis
- QUANTIFICATION AND STATISTICAL ANALYSIS

SUPPLEMENTAL INFORMATION

Supplemental information can be found online at https://doi.org/10.1016/j.isci.2025.112030.

Received: March 4, 2024
Revised: November 28, 2024
Accepted: February 11, 2025
Published: February 14, 2025

REFERENCES

1. Tisdale, M.J. (2002). Cachexia in cancer patients. Nat. Rev. Cancer *2*, 862–871. https://doi.org/10.1038/nrc927.
2. Tisdale, M.J. (2003). The "cancer cachectic factor.". Support. Care Cancer *11*, 73–78. https://doi.org/10.1007/s00520-002-0408-6.
3. Fearon, K., Strasser, F., Anker, S.D., Bosaeus, I., Bruera, E., Fainsinger, R.L., Jatoi, A., Loprinzi, C., MacDonald, N., Mantovani, G., et al. (2011). Definition and classification of cancer cachexia: an international consensus. Lancet Oncol. *12*, 489–495. https://doi.org/10.1016/S1470-2045(10)70218-7.
4. Baracos, V.E., Martin, L., Korc, M., Guttridge, D.C., and Fearon, K.C.H. (2018). Cancer-associated cachexia. Nat. Rev. Dis. Primers *4*, 17105. https://doi.org/10.1038/nrdp.2017.105.
5. Ferrer, M., Anthony, T.G., Ayres, J.S., Biffi, G., Brown, J.C., Caan, B.J., Cespedes Feliciano, E.M., Coll, A.P., Dunne, R.F., Goncalves, M.D., et al. (2023). Cachexia: A systemic consequence of progressive, unresolved disease. Cell *186*, 1824–1845. https://doi.org/10.1016/j.cell.2023.03.028.
6. Rohm, M., Zeigerer, A., Machado, J., and Herzig, S. (2019). Energy metabolism in cachexia. EMBO Rep. *20*, e47258. https://doi.org/10.15252/embr.201847258.
7. Argilés, J.M., López-Soriano, F.J., Stemmler, B., and Busquets, S. (2023). Cancer-associated cachexia - understanding the tumour macroenvironment and microenvironment to improve management. Nat. Rev. Clin. Oncol. *20*, 250–264. https://doi.org/10.1038/s41571-023-00734-5.
8. Fearon, K.C.H., Glass, D.J., and Guttridge, D.C. (2012). Cancer cachexia: mediators, signaling, and metabolic pathways. Cell Metab. *16*, 153–166. https://doi.org/10.1016/j.cmet.2012.06.011.
9. Siddiqui, J.A., Pothuraju, R., Jain, M., Batra, S.K., and Nasser, M.W. (2020). Advances in cancer cachexia: Intersection between affected organs, mediators, and pharmacological interventions. Biochim. Biophys. Acta Rev. Canc *1873*, 188359. https://doi.org/10.1016/j.bbcan.2020.188359.
10. Argilés, J.M., Busquets, S., and López-Soriano, F.J. (2003). Cytokines in the pathogenesis of cancer cachexia. Curr. Opin. Clin. Nutr. Metab. Care *6*, 401–406. https://doi.org/10.1097/01.mco.0000078983.18774.cc.
11. Laird, B.J., McMillan, D., Skipworth, R.J.E., Fallon, M.T., Paval, D.R., McNeish, I., and Gallagher, I.J. (2021). The Emerging Role of Interleukin 1β (IL-1β) in Cancer Cachexia. Inflammation *44*, 1223–1228. https://doi.org/10.1007/s10753-021-01429-8.
12. Balsano, R., Kruize, Z., Lunardi, M., Comandatore, A., Barone, M., Cavazzoni, A., Re Cecconi, A.D., Morelli, L., Wilmink, H., Tiseo, M., et al. (2022). Transforming Growth Factor-Beta Signaling in Cancer-Induced Cachexia: From Molecular Pathways to the Clinics. Cells *11*, 2671. https://doi.org/10.3390/cells11172671.
13. Talbert, E.E., and Guttridge, D.C. (2022). Emerging signaling mediators in the anorexia–cachexia syndrome of cancer. Trends Cancer *8*, 397–403. https://doi.org/10.1016/j.trecan.2022.01.004.
14. Suzuki, H., Mitsunaga, S., Ikeda, M., Aoyama, T., Yoshizawa, K., Yoshimatsu, H., Kawai, N., Masuda, M., Miura, T., and Ochiai, A. (2021). Clinical and Tumor Characteristics of Patients with High Serum Levels of Growth Differentiation Factor 15 in Advanced Pancreatic Cancer. Cancers *13*, 4842. https://doi.org/10.3390/cancers13194842.
15. Rupert, J.E., Narasimhan, A., Jengelley, D.H.A., Jiang, Y., Liu, J., Au, E., Silverman, L.M., Sandusky, G., Bonetto, A., Cao, S., et al. (2021). Tumor-derived IL-6 and trans-signaling among tumor, fat, and muscle mediate pancreatic cancer cachexia. J. Exp. Med. *218*, e20190450. https://doi.org/10.1084/jem.20190450.
16. Schöbitz, B., Pezeshki, G., Pohl, T., Hemmann, U., Heinrich, P.C., Holsboer, F., and Reul, J.M. (1995). Soluble interleukin-6 (IL-6) receptor augments central effects of IL-6 in vivo. FASEB J. *9*, 659–664. https://doi.org/10.1096/fasebj.9.8.7768358.
17. Bonetto, A., Aydogdu, T., Jin, X., Zhang, Z., Zhan, R., Puzis, L., Koniaris, L.G., and Zimmers, T.A. (2012). JAK/STAT3 pathway inhibition blocks skeletal muscle wasting downstream of IL-6 and in experimental cancer cachexia. Am. J. Physiol. Endocrinol. Metab. *303*, E410–E421. https://doi.org/10.1152/ajpendo.00039.2012.
18. Chen, J.L., Walton, K.L., Qian, H., Colgan, T.D., Hagg, A., Watt, M.J., Harrison, C.A., and Gregorevic, P. (2016). Differential Effects of IL6 and Activin A in the Development of Cancer-Associated Cachexia. Cancer Res. *76*, 5372–5382. https://doi.org/10.1158/0008-5472.CAN-15-3152.
19. Bindels, L.B., Neyrinck, A.M., Loumaye, A., Catry, E., Walgrave, H., Cherbuy, C., Leclercq, S., Van Hul, M., Plovier, H., Pachikian, B., et al. (2018). Increased gut permeability in cancer cachexia: mechanisms and clinical relevance. Oncotarget *9*, 18224–18238. https://doi.org/10.18632/oncotarget.24804.
20. Lerner, L., Tao, J., Liu, Q., Nicoletti, R., Feng, B., Krieger, B., Mazsa, E., Siddiquee, Z., Wang, R., Huang, L., et al. (2016). MAP3K11/GDF15 axis is a critical driver of cancer cachexia. J. Cachexia Sarcopenia Muscle *7*, 467–482. https://doi.org/10.1002/jcsm.12077.
21. Johnen, H., Lin, S., Kuffner, T., Brown, D.A., Tsai, V.W.-W., Bauskin, A.R., Wu, L., Pankhurst, G., Jiang, L., Junankar, S., et al. (2007). Tumor-induced anorexia and weight loss are mediated by the TGF-beta superfamily cytokine MIC-1. Nat. Med. *13*, 1333–1340. https://doi.org/10.1038/nm1677.
22. Suriben, R., Chen, M., Higbee, J., Oeffinger, J., Ventura, R., Li, B., Mondal, K., Gao, Z., Ayupova, D., Taskar, P., et al. (2020). Antibody-mediated inhibition of GDF15–GFRAL activity reverses cancer cachexia in mice. Nat. Med. *26*, 1264–1270. https://doi.org/10.1038/s41591-020-0945-x.
23. Hinnebusch, A.G., Ivanov, I.P., and Sonenberg, N. (2016). Translational control by 5'-untranslated regions of eukaryotic mRNAs. Science *352*, 1413–1416. https://doi.org/10.1126/science.aad9868.
24. Pakos-Zebrucka, K., Koryga, I., Mnich, K., Ljujic, M., Samali, A., and Gorman, A.M. (2016). The integrated stress response. EMBO Rep. *17*, 1374–1395. https://doi.org/10.15252/embr.201642195.
25. Wek, R.C., Anthony, T.G., and Staschke, K.A. (2023). Surviving and Adapting to Stress: Translational Control and the Integrated Stress Response. Antioxidants Redox Signal. *39*, 351–373. https://doi.org/10.1089/ars.2022.0123.
26. Harding, H.P., Novoa, I., Zhang, Y., Zeng, H., Wek, R., Schapira, M., and Ron, D. (2000). Regulated translation initiation controls stress-induced gene expression in mammalian cells. Mol. Cell *6*, 1099–1108. https://doi.org/10.1016/s1097-2765(00)00108-8.
27. Kilberg, M.S., Shan, J., and Su, N. (2009). ATF4-dependent transcription mediates signaling of amino acid limitation. Trends Endocrinol. Metabol. *20*, 436–443. https://doi.org/10.1016/j.tem.2009.05.008.
28. Quirós, P.M., Prado, M.A., Zamboni, N., D'Amico, D., Williams, R.W., Finley, D., Gygi, S.P., and Auwerx, J. (2017). Multi-omics analysis identifies ATF4 as a key regulator of the mitochondrial stress response in mammals. J. Cell Biol. *216*, 2027–2045. https://doi.org/10.1083/jcb.201702058.
29. B'chir, W., Maurin, A.-C., Carraro, V., Averous, J., Jousse, C., Muranishi, Y., Parry, L., Stepien, G., Fafournoux, P., and Bruhat, A. (2013). The eIF2α/ATF4 pathway is essential for stress-induced autophagy gene expression. Nucleic Acids Res. *41*, 7683–7699. https://doi.org/10.1093/nar/gkt563.

30. Neill, G., and Masson, G.R. (2023). A stay of execution: ATF4 regulation and potential outcomes for the integrated stress response. Front. Mol. Neurosci. *16*, 1112253. https://doi.org/10.3389/fnmol.2023.1112253.

31. Hao, S., Sharp, J.W., Ross-Inta, C.M., McDaniel, B.J., Anthony, T.G., Wek, R.C., Cavener, D.R., McGrath, B.C., Rudell, J.B., Koehnle, T.J., and Gietzen, D.W. (2005). Uncharged tRNA and sensing of amino acid deficiency in mammalian piriform cortex. Science *307*, 1776–1778. https://doi.org/10.1126/science.1104882.

32. Maurin, A.C., Jousse, C., Averous, J., Parry, L., Bruhat, A., Cherasse, Y., Zeng, H., Zhang, Y., Harding, H.P., Ron, D., and Fafournoux, P. (2005). The GCN2 kinase biases feeding behavior to maintain amino acid homeostasis in omnivores. Cell Metab. *1*, 273–277. https://doi.org/10.1016/j.cmet.2005.03.004.

33. Maurin, A.-C., Benani, A., Lorsignol, A., Brenachot, X., Parry, L., Carraro, V., Guissard, C., Averous, J., Jousse, C., Bruhat, A., et al. (2014). Hypothalamic eIF2α signaling regulates food intake. Cell Rep. *6*, 438–444. https://doi.org/10.1016/j.celrep.2014.01.006.

34. Bjordal, M., Arquier, N., Kniazeff, J., Pin, J.P., and Léopold, P. (2014). Sensing of amino acids in a dopaminergic circuitry promotes rejection of an incomplete diet in Drosophila. Cell *156*, 510–521. https://doi.org/10.1016/j.cell.2013.12.024.

35. Ravindran, R., Loebbermann, J., Nakaya, H.I., Khan, N., Ma, H., Gama, L., Machiah, D.K., Lawson, B., Hakimpour, P., Wang, Y.-C., et al. (2016). The amino acid sensor GCN2 controls gut inflammation by inhibiting inflammasome activation. Nature *531*, 523–527. https://doi.org/10.1038/nature17186.

36. Ye, J., Kumanova, M., Hart, L.S., Sloane, K., Zhang, H., De Panis, D.N., Bobrovnikova-Marjon, E., Diehl, J.A., Ron, D., and Koumenis, C. (2010). The GCN2-ATF4 pathway is critical for tumour cell survival and proliferation in response to nutrient deprivation. EMBO J. *29*, 2082–2096. https://doi.org/10.1038/emboj.2010.81.

37. Maurin, A.-C., Parry, L., B'chir, W., Carraro, V., Coudy-Gandilhon, C., Chaouki, G., Chaveroux, C., Mordier, S., Martinie, B., Reinhardt, V., et al. (2022). GCN2 upregulates autophagy in response to short-term deprivation of a single essential amino acid. Autoph. Rep. *1*, 119–142. https://doi.org/10.1080/27694127.2022.2049045.

38. Tanaka, Y., Eda, H., Tanaka, T., Udagawa, T., Ishikawa, T., Horii, I., Ishitsuka, H., Kataoka, T., and Taguchi, T. (1990). Experimental cancer cachexia induced by transplantable colon 26 adenocarcinoma in mice. Cancer Res. *50*, 2290–2295.

39. Yeom, E., Shin, H., Yoo, W., Jun, E., Kim, S., Hong, S.H., Kwon, D.-W., Ryu, T.H., Suh, J.M., Kim, S.C., et al. (2021). Tumour-derived Dilp8/INSL3 induces cancer anorexia by regulating feeding neuropeptides via Lgr3/8 in the brain. Nat. Cell Biol. *23*, 172–183. https://doi.org/10.1038/s41556-020-00628-z.

40. Bodine, S.C., Latres, E., Baumhueter, S., Lai, V.K., Nunez, L., Clarke, B.A., Poueymirou, W.T., Panaro, F.J., Na, E., Dharmarajan, K., et al. (2001). Identification of ubiquitin ligases required for skeletal muscle atrophy. Science *294*, 1704–1708. https://doi.org/10.1126/science.1065874.

41. Jagoe, R.T., Lecker, S.H., Gomes, M., and Goldberg, A.L. (2002). Patterns of gene expression in atrophying skeletal muscles: response to food deprivation. FASEB J. *16*, 1697–1712. https://doi.org/10.1096/fj.02-0312com.

42. Lecker, S.H., Jagoe, R.T., Gilbert, A., Gomes, M., Baracos, V., Bailey, J., Price, S.R., Mitch, W.E., and Goldberg, A.L. (2004). Multiple types of skeletal muscle atrophy involve a common program of changes in gene expression. FASEB J. *18*, 39–51. https://doi.org/10.1096/fj.03-0610com.

43. Taillandier, D., and Polge, C. (2019). Skeletal muscle atrogenes: From rodent models to human pathologies. Biochimie *166*, 251–269. https://doi.org/10.1016/j.biochi.2019.07.014.

44. Ezeoke, C.C., and Morley, J.E. (2015). Pathophysiology of anorexia in the cancer cachexia syndrome. J. Cachexia Sarcopenia Muscle *6*, 287–302. https://doi.org/10.1002/jcsm.12059.

45. Chance, W.T., Sheriff, S., Kasckow, J.W., Regmi, A., and Balasubramaniam, A. (1998). NPY messenger RNA is increased in medial hypothalamus of anorectic tumor-bearing rats. Regul. Pept. *75–76*, 347–353. https://doi.org/10.1016/s0167-0115(98)00087-1.

46. Nara-ashizawa, N., Tsukada, T., Maruyama, K., Akiyama, Y., Kajimura, N., Nagasaki, K., Iwanaga, T., and Yamaguchi, K. (2001). Hypothalamic appetite-regulating neuropeptide mRNA levels in cachectic nude mice bearing human tumor cells. Metabolism *50*, 1213–1219. https://doi.org/10.1053/meta.2001.26706.

47. Nara-ashizawa, N., Tsukada, T., Maruyama, K., Akiyama, Y., Kajimura, N., and Yamaguchi, K. (2001). Response of hypothalamic NPY mRNAs to a negative energy balance is less sensitive in cachectic mice bearing human tumor cells. Nutr. Cancer *41*, 111–118. https://doi.org/10.1080/01635581.2001.9680621.

48. Krasnow, S.M., and Marks, D.L. (2010). Neuropeptides in the pathophysiology and treatment of cachexia. Curr. Opin. Support. Palliat. Care *4*, 266–271. https://doi.org/10.1097/SPC.0b013e32833e48e7.

49. Huisman, C., Norgard, M.A., Levasseur, P.R., Krasnow, S.M., van der Wijst, M.G.P., Olson, B., and Marks, D.L. (2022). Critical changes in hypothalamic gene networks in response to pancreatic cancer as found by single-cell RNA sequencing. Mol. Metabol. *58*, 101441. https://doi.org/10.1016/j.molmet.2022.101441.

50. Villars, F.O., Pietra, C., Giuliano, C., Lutz, T.A., and Riediger, T. (2017). Oral Treatment with the Ghrelin Receptor Agonist HM01 Attenuates Cachexia in Mice Bearing Colon-26 (C26) Tumors. Int. J. Mol. Sci. *18*, 986. https://doi.org/10.3390/ijms18050986.

51. Geppert, J., Walth, A.A., Terrón Expósito, R., Kaltenecker, D., Morigny, P., Machado, J., Becker, M., Simoes, E., Lima, J.D.C.C., Daniel, C., et al. (2021). Aging Aggravates Cachexia in Tumor-Bearing Mice. Cancers *14*, 90. https://doi.org/10.3390/cancers14010090.

52. Argilés, J.M., Stemmler, B., López-Soriano, F.J., and Busquets, S. (2019). Inter-tissue communication in cancer cachexia. Nat. Rev. Endocrinol. *15*, 9–20. https://doi.org/10.1038/s41574-018-0123-0.

53. de Blaauw, I., Heeneman, S., Deutz, N.E., and von Meyenfeldt, M.F. (1997). Increased whole-body protein and glutamine turnover in advanced cancer is not matched by an increased muscle protein and glutamine turnover. J. Surg. Res. *68*, 44–55. https://doi.org/10.1006/jsre.1997.5007.

54. de Blaauw, I., Deutz, N.E., Boers, W., and von Meyenfeldt, M.F. (1997). Hepatic amino acid and protein metabolism in non-anorectic, moderately cachectic tumor-bearing rats. J. Hepatol. *26*, 396–408. https://doi.org/10.1016/s0168-8278(97)80058-x.

55. Bonetto, A., Rupert, J.E., Barreto, R., and Zimmers, T.A. (2016). The Colon-26 Carcinoma Tumor-bearing Mouse as a Model for the Study of Cancer Cachexia. J. Vis. Exp. *54893*, 54893. https://doi.org/10.3791/54893.

56. Zimmers, T.A., Fishel, M.L., and Bonetto, A. (2016). STAT3 in the systemic inflammation of cancer cachexia. Semin. Cell Dev. Biol. *54*, 28–41. https://doi.org/10.1016/j.semcdb.2016.02.009.

57. Rose-John, S. (2022). Local and systemic effects of interleukin-6 (IL-6) in inflammation and cancer. FEBS Lett. *596*, 557–566. https://doi.org/10.1002/1873-3468.14220.

58. Bode, J.G., Albrecht, U., Häussinger, D., Heinrich, P.C., and Schaper, F. (2012). Hepatic acute phase proteins–regulation by IL-6- and IL-1-type cytokines involving STAT3 and its crosstalk with NF-κB-dependent signaling. Eur. J. Cell Biol. *91*, 496–505. https://doi.org/10.1016/j.ejcb.2011.09.008.

59. Zhang, D., Sun, M., Samols, D., and Kushner, I. (1996). STAT3 Participates in Transcriptional Activation of the C-reactive Protein Gene by Interleukin-6 (*). J. Biol. Chem. *271*, 9503–9509. https://doi.org/10.1074/jbc.271.16.9503.

60. Zhong, Z., Wen, Z., and Darnell, J.E. (1994). Stat3: a STAT family member activated by tyrosine phosphorylation in response to epidermal growth

factor and interleukin-6. Science *264*, 95–98. https://doi.org/10.1126/science.8140422.

61. Schindler, C., and Darnell, J.E. (1995). Transcriptional responses to polypeptide ligands: the JAK-STAT pathway. Annu. Rev. Biochem. *64*, 621–651. https://doi.org/10.1146/annurev.bi.64.070195.003201.

62. Laplante, M., and Sabatini, D.M. (2012). mTOR Signaling in Growth Control and Disease. Cell *149*, 274–293. https://doi.org/10.1016/j.cell.2012.03.017.

63. Paulusma, C.C., Lamers, W.H., Broer, S., and van de Graaf, S.F.J. (2022). Amino acid metabolism, transport and signalling in the liver revisited. Biochem. Pharmacol. *201*, 115074. https://doi.org/10.1016/j.bcp.2022.115074.

64. Cray, C., Zaias, J., and Altman, N.H. (2009). Acute phase response in animals: a review. Comp. Med. *59*, 517–526.

65. Mantovani, A., and Garlanda, C. (2023). Humoral Innate Immunity and Acute-Phase Proteins. N. Engl. J. Med. *388*, 439–452. https://doi.org/10.1056/NEJMra2206346.

66. Ehlting, C., Wolf, S.D., and Bode, J.G. (2021). Acute-phase protein synthesis: a key feature of innate immune functions of the liver. Biol. Chem. *402*, 1129–1145. https://doi.org/10.1515/hsz-2021-0209.

67. Heinrich, P.C., Castell, J.V., and Andus, T. (1990). Interleukin-6 and the acute phase response. Biochem. J. *265*, 621–636. https://doi.org/10.1042/bj2650621.

68. Betts, J.C., Cheshire, J.K., Akira, S., Kishimoto, T., and Woo, P. (1993). The role of NF-kappa B and NF-IL6 transactivating factors in the synergistic activation of human serum amyloid A gene expression by interleukin-1 and interleukin-6. J. Biol. Chem. *268*, 25624–25631.

69. Thorn, C.F., Lu, Z.-Y., and Whitehead, A.S. (2004). Regulation of the human acute phase serum amyloid A genes by tumour necrosis factor-alpha, interleukin-6 and glucocorticoids in hepatic and epithelial cell lines. Scand. J. Immunol. *59*, 152–158. https://doi.org/10.1111/j.0300-9475.2004.01369.x.

70. Castell, J.V., Gómez-Lechón, M.J., David, M., Fabra, R., Trullenque, R., and Heinrich, P.C. (1990). Acute-phase response of human hepatocytes: regulation of acute-phase protein synthesis by interleukin-6. Hepatology *12*, 1179–1186. https://doi.org/10.1002/hep.1840120517.

71. Bharadwaj, U., Kasembeli, M.M., Robinson, P., and Tweardy, D.J. (2020). Targeting Janus Kinases and Signal Transducer and Activator of Transcription 3 to Treat Inflammation, Fibrosis, and Cancer: Rationale, Progress, and Caution. Pharmacol. Rev. *72*, 486–526. https://doi.org/10.1124/pr.119.018440.

72. Hagihara, K., Nishikawa, T., Sugamata, Y., Song, J., Isobe, T., Taga, T., and Yoshizaki, K. (2005). Essential role of STAT3 in cytokine-driven NF-kappaB-mediated serum amyloid A gene expression. Genes Cells *10*, 1051–1063. https://doi.org/10.1111/j.1365-2443.2005.00900.x.

73. Bonetto, A., Aydogdu, T., Kunzevitzky, N., Guttridge, D.C., Khuri, S., Koniaris, L.G., and Zimmers, T.A. (2011). STAT3 activation in skeletal muscle links muscle wasting and the acute phase response in cancer cachexia. PLoS One *6*, e22538. https://doi.org/10.1371/journal.pone.0022538.

74. Jang, C., Hui, S., Zeng, X., Cowan, A.J., Wang, L., Chen, L., Morscher, R.J., Reyes, J., Frezza, C., Hwang, H.Y., et al. (2019). Metabolite Exchange between Mammalian Organs Quantified in Pigs. Cell Metab. *30*, 594–606. https://doi.org/10.1016/j.cmet.2019.06.002.

75. Wester, T.J., Kraft, G., Dardevet, D., Polakof, S., Ortigues-Marty, I., Rémond, D., and Savary-Auzeloux, I. (2015). Nutritional regulation of the anabolic fate of amino acids within the liver in mammals: concepts arising from in vivo studies. Nutr. Res. Rev. *28*, 22–41. https://doi.org/10.1017/S0954422415000013.

76. Mortimore, G.E., and Schworer, C.M. (1977). Induction of autophagy by amino-acid deprivation in perfused rat liver. Nature *270*, 174–176.

77. Mortimore, G.E., and Pösö, A.R. (1987). Intracellular protein catabolism and its control during nutrient deprivation and supply. Annu. Rev. Nutr. *7*, 539–564. https://doi.org/10.1146/annurev.nu.07.070187.002543.

78. Komatsu, M., Waguri, S., Ueno, T., Iwata, J., Murata, S., Tanida, I., Ezaki, J., Mizushima, N., Ohsumi, Y., Uchiyama, Y., et al. (2005). Impairment of starvation-induced and constitutive autophagy in Atg7-deficient mice. J. Cell Biol. *169*, 425–434. https://doi.org/10.1083/jcb.200412022.

79. Ganley, I.G., Lam, D.H., Wang, J., Ding, X., Chen, S., and Jiang, X. (2009). ULK1.ATG13.FIP200 complex mediates mTOR signaling and is essential for autophagy. J. Biol. Chem. *284*, 12297–12305. https://doi.org/10.1074/jbc.M900573200.

80. Hosokawa, N., Hara, T., Kaizuka, T., Kishi, C., Takamura, A., Miura, Y., Iemura, S.i., Natsume, T., Takehana, K., Yamada, N., et al. (2009). Nutrient-dependent mTORC1 association with the ULK1-Atg13-FIP200 complex required for autophagy. Mol. Biol. Cell *20*, 1981–1991. https://doi.org/10.1091/mbc.E08-12-1248.

81. Kim, J., Kundu, M., Viollet, B., and Guan, K.L. (2011). AMPK and mTOR regulate autophagy through direct phosphorylation of Ulk1. Nat. Cell Biol. *13*, 132–141. https://doi.org/10.1038/ncb2152.

82. Deleyto-Seldas, N., and Efeyan, A. (2021). The mTOR-Autophagy Axis and the Control of Metabolism. Front. Cell Dev. Biol. *9*, 655731. https://doi.org/10.3389/fcell.2021.655731.

83. Nazio, F., Carinci, M., Valacca, C., Bielli, P., Strappazzon, F., Antonioli, M., Ciccosanti, F., Rodolfo, C., Campello, S., Fimia, G.M., et al. (2016). Fine-tuning of ULK1 mRNA and protein levels is required for autophagy oscillation. J. Cell Biol. *215*, 841–856. https://doi.org/10.1083/jcb.201605089.

84. Goldberg, A.A., Nkengfac, B., Sanchez, A.M.J., Moroz, N., Qureshi, S.T., Koromilas, A.E., Wang, S., Burelle, Y., Hussain, S.N., and Kristof, A.S. (2017). Regulation of ULK1 Expression and Autophagy by STAT1. J. Biol. Chem. *292*, 1899–1909. https://doi.org/10.1074/jbc.M116.771584.

85. Han, J., Back, S.H., Hur, J., Lin, Y.-H., Gildersleeve, R., Shan, J., Yuan, C.L., Krokowski, D., Wang, S., Hatzoglou, M., et al. (2013). ER-stress-induced transcriptional regulation increases protein synthesis leading to cell death. Nat. Cell Biol. *15*, 481–490. https://doi.org/10.1038/ncb2738.

86. Palii, S.S., Thiaville, M.M., Pan, Y.-X., Zhong, C., and Kilberg, M.S. (2006). Characterization of the amino acid response element within the human sodium-coupled neutral amino acid transporter 2 (SNAT2) System A transporter gene. Biochem. J. *395*, 517–527. https://doi.org/10.1042/BJ20051867.

87. He, F., Zhang, P., Liu, J., Wang, R., Kaufman, R.J., Yaden, B.C., and Karin, M. (2023). ATF4 suppresses hepatocarcinogenesis by inducing SLC7A11 (xCT) to block stress-related ferroptosis. J. Hepatol. *79*, 362–377. https://doi.org/10.1016/j.jhep.2023.03.016.

88. Siu, F., Bain, P.J., LeBlanc-Chaffin, R., Chen, H., and Kilberg, M.S. (2002). ATF4 is a mediator of the nutrient-sensing response pathway that activates the human asparagine synthetase gene. J. Biol. Chem. *277*, 24120–24127. https://doi.org/10.1074/jbc.M201959200.

89. Strassmann, G., Jacob, C.O., Evans, R., Beall, D., and Fong, M. (1992). Mechanisms of experimental cancer cachexia. Interaction between mononuclear phagocytes and colon-26 carcinoma and its relevance to IL-6-mediated cancer cachexia. J. Immunol. *148*, 3674–3678.

90. Welsh, J.B., Sapinoso, L.M., Kern, S.G., Brown, D.A., Liu, T., Bauskin, A.R., Ward, R.L., Hawkins, N.J., Quinn, D.I., Russell, P.J., et al. (2003). Large-scale delineation of secreted protein biomarkers overexpressed in cancer tissue and serum. Proc. Natl. Acad. Sci. USA *100*, 3410–3415. https://doi.org/10.1073/pnas.0530278100.

91. Greten, F.R., and Grivennikov, S.I. (2019). Inflammation and Cancer: Triggers, Mechanisms, and Consequences. Immunity *51*, 27–41. https://doi.org/10.1016/j.immuni.2019.06.025.

92. Aguilar-Recarte, D., Barroso, E., Palomer, X., Wahli, W., and Vázquez-Carrera, M. (2022). Knocking on GDF15's door for the treatment of

type 2 diabetes mellitus. Trends Endocrinol. Metabol. *33*, 741–754. https://doi.org/10.1016/j.tem.2022.08.004.

93. Klein, A.B., Nicolaisen, T.S., Ørtenblad, N., Gejl, K.D., Jensen, R., Fritzen, A.M., Larsen, E.L., Karstoft, K., Poulsen, H.E., Morville, T., et al. (2021). Pharmacological but not physiological GDF15 suppresses feeding and the motivation to exercise. Nat. Commun. *12*, 1041. https://doi.org/10.1038/s41467-021-21309-x.
94. Ost, M., Igual Gil, C., Coleman, V., Keipert, S., Efstathiou, S., Vidic, V., Weyers, M., and Klaus, S. (2020). Muscle-derived GDF15 drives diurnal anorexia and systemic metabolic remodeling during mitochondrial stress. EMBO Rep. *21*, e48804. https://doi.org/10.15252/embr.201948804.
95. Sigvardsen, C.M., Richter, M.M., Engelbeen, S., Kleinert, M., and Richter, E.A. (2024). GDF15 is still a mystery hormone. Trends Endocrinol. Metabol. https://doi.org/10.1016/j.tem.2024.09.002.
96. Beck, S.A., and Tisdale, M.J. (1989). Nitrogen excretion in cancer cachexia and its modification by a high fat diet in mice. Cancer Res. *49*, 3800–3804.
97. Pötgens, S.A., Thibaut, M.M., Joudiou, N., Sboarina, M., Neyrinck, A.M., Cani, P.D., Claus, S.P., Delzenne, N.M., and Bindels, L.B. (2021). Multi-compartment metabolomics and metagenomics reveal major hepatic and intestinal disturbances in cancer cachectic mice. J. Cachexia Sarcopenia Muscle *12*, 456–475. https://doi.org/10.1002/jcsm.12684.
98. Der-Torossian, H., Asher, S.A., Winnike, J.H., Wysong, A., Yin, X., Willis, M.S., O'Connell, T.M., and Couch, M.E. (2013). Cancer cachexia's metabolic signature in a murine model confirms a distinct entity. Metabolomics *9*, 730–739. https://doi.org/10.1007/s11306-012-0485-6.
99. O'Connell, T.M., Golzarri-Arroyo, L., Pin, F., Barreto, R., Dickinson, S.L., Couch, M.E., and Bonetto, A. (2021). Metabolic Biomarkers for the Early Detection of Cancer Cachexia. Front. Cell Dev. Biol. *9*, 720096. https://doi.org/10.3389/fcell.2021.720096.
100. Mercier, S., Breuillé, D., Mosoni, L., Obled, C., and Patureau Mirand, P. (2002). Chronic inflammation alters protein metabolism in several organs of adult rats. J. Nutr. *132*, 1921–1928. https://doi.org/10.1093/jn/132.7.1921.
101. Obled, C. (2003). Amino acid requirements in inflammatory states. Can. J. Anim. Sci. *83*, 365–373. https://doi.org/10.4141/A03-021.
102. Lundholm, K., Edström, S., Ekman, L., Karlberg, I., Bylund, A.C., and Scherstén, T. (1978). A comparative study of the influence of malignant tumor on host metabolism in mice and man: evaluation of an experimental model. Cancer *42*, 453–461. https://doi.org/10.1002/1097-0142(197808)42:2<453::aid-cncr2820420212>3.0.co;2-t.
103. Douglas, R.G., and Shaw, J.H. (1990). Metabolic effects of cancer. Br. J. Surg. *77*, 246–254. https://doi.org/10.1002/bjs.1800770305.
104. Norton, J.A., Shamberger, R., Stein, T.P., Milne, G.W., and Brennan, M.F. (1981). The influence of tumor-bearing on protein metabolism in the rat. J. Surg. Res. *30*, 456–462. https://doi.org/10.1016/0022-4804(81)90090-1.
105. Samuels, S.E., McLaren, T.A., Knowles, A.L., Stewart, S.A., Madelmont, J.-C., and Attaix, D. (2006). Liver protein synthesis stays elevated after chemotherapy in tumour-bearing mice. Cancer Lett. *239*, 78–83. https://doi.org/10.1016/j.canlet.2005.07.026.
106. Lautaoja, J.H., Lalowski, M., Nissinen, T.A., Hentilä, J., Shi, Y., Ritvos, O., Cheng, S., and Hulmi, J.J. (2019). Muscle and serum metabolomes are dysregulated in colon-26 tumor-bearing mice despite amelioration of cachexia with activin receptor type 2B ligand blockade. Am. J. Physiol. Endocrinol. Metab. *316*, E852–E865. https://doi.org/10.1152/ajpendo.00526.2018.
107. Reeds, P.J. (2000). Dispensable and indispensable amino acids for humans. J. Nutr. *130*, 1835S–1840S. https://doi.org/10.1093/jn/130.7.1835S.
108. Ruot, B., Béchereau, F., Bayle, G., Breuillé, D., and Obled, C. (2002). The response of liver albumin synthesis to infection in rats varies with the phase of the inflammatory process. Clin. Sci. *102*, 107–114.
109. Castillo, A.M.M., Vu, T.T., Liva, S.G., Chen, M., Xie, Z., Thomas, J., Remaily, B., Guo, Y., Subrayan, U.L., Costa, T., et al. (2021). Murine cancer cachexia models replicate elevated catabolic pembrolizumab clearance in humans. JCSM Rapid Commun. *4*, 232–244. https://doi.org/10.1002/rco2.32.
110. Brenner, D.A., Buck, M., Feitelberg, S.P., and Chojkier, M. (1990). Tumor necrosis factor-alpha inhibits albumin gene expression in a murine model of cachexia. J. Clin. Investig. *85*, 248–255. https://doi.org/10.1172/JCI114419.
111. Trautwein, C., Rakemann, T., Pietrangelo, A., Plümpe, J., Montosi, G., and Manns, M.P. (1996). C/EBP-β/LAP Controls Down-regulation of Albumin Gene Transcription during Liver Regeneration. J. Biol. Chem. *271*, 22262–22270. https://doi.org/10.1074/jbc.271.36.22262.
112. Chojkier, M. (2005). Inhibition of albumin synthesis in chronic diseases: molecular mechanisms. J. Clin. Gastroenterol. *39*, S143–S146. https://doi.org/10.1097/01.mcg.0000155514.17715.39.
113. Vary, T.C., and Kimball, S.R. (1992). Regulation of hepatic protein synthesis in chronic inflammation and sepsis. Am. J. Physiol. *262*, C445–C452. https://doi.org/10.1152/ajpcell.1992.262.2.C445.
114. Gabay, C., and Kushner, I. (1999). Acute-phase proteins and other systemic responses to inflammation. N. Engl. J. Med. *340*, 448–454. https://doi.org/10.1056/NEJM199902113400607.
115. Robinson, T.P., Hamidi, T., Counts, B., Guttridge, D.C., Ostrowski, M.C., Zimmers, T.A., and Koniaris, L.G. (2023). The impact of inflammation and acute phase activation in cancer cachexia. Front. Immunol. *14*, 1207746. https://doi.org/10.3389/fimmu.2023.1207746.
116. Fearon, K.C., Barber, M.D., Falconer, J.S., McMillan, D.C., Ross, J.A., and Preston, T. (1999). Pancreatic cancer as a model: inflammatory mediators, acute-phase response, and cancer cachexia. World J. Surg. *23*, 584–588. https://doi.org/10.1007/pl00012351.
117. Chaveroux, C., Carraro, V., Canaple, L., Averous, J., Maurin, A.-C., Jousse, C., Muranishi, Y., Parry, L., Mesclon, F., Gatti, E., et al. (2015). In vivo imaging of the spatiotemporal activity of the eIF2α-ATF4 signaling pathway: Insights into stress and related disorders. Sci. Signal. *8*, rs5. https://doi.org/10.1126/scisignal.aaa0549.
118. Jonsson, W.O., Mirek, E.T., Wek, R.C., and Anthony, T.G. (2022). Activation and execution of the hepatic integrated stress response by dietary essential amino acid deprivation is amino acid specific. FASEB J. *36*, e22396. https://doi.org/10.1096/fj.202200204RR.
119. Chaveroux, C., Bruhat, A., Carraro, V., Jousse, C., Averous, J., Maurin, A.C., Parry, L., Mesclon, F., Muranishi, Y., Cordelier, P., et al. (2016). Regulating the expression of therapeutic transgenes by controlled intake of dietary essential amino acids. Nat. Biotechnol. *34*, 746–751. https://doi.org/10.1038/nbt.3582.
120. Hentilä, J., Nissinen, T.A., Korkmaz, A., Lensu, S., Silvennoinen, M., Pasternack, A., Ritvos, O., Atalay, M., and Hulmi, J.J. (2018). Activin Receptor Ligand Blocking and Cancer Have Distinct Effects on Protein and Redox Homeostasis in Skeletal Muscle and Liver. Front. Physiol. *9*, 1917. https://doi.org/10.3389/fphys.2018.01917.
121. White, E., Lattime, E.C., and Guo, J.Y. (2021). Autophagy Regulates Stress Responses, Metabolism, and Anticancer Immunity. Trends Cancer *7*, 778–789. https://doi.org/10.1016/j.trecan.2021.05.003.
122. Kroemer, G., Mariño, G., and Levine, B. (2010). Autophagy and the integrated stress response. Mol. Cell *40*, 280–293. https://doi.org/10.1016/j.molcel.2010.09.023.
123. Nissinen, T.A., Hentilä, J., Penna, F., Lampinen, A., Lautaoja, J.H., Fachada, V., Holopainen, T., Ritvos, O., Kivelä, R., and Hulmi, J.J. (2018). Treating cachexia using soluble ACVR2B improves survival, alters mTOR localization, and attenuates liver and spleen responses. J. Cachexia Sarcopenia Muscle *9*, 514–529. https://doi.org/10.1002/jcsm.12310.
124. Fearon, K.C., McMillan, D.C., Preston, T., Winstanley, F.P., Cruickshank, A.M., and Shenkin, A. (1991). Elevated circulating interleukin-6 is associated with an acute-phase response but reduced fixed hepatic protein

synthesis in patients with cancer. Ann. Surg. *213*, 26–31. https://doi.org/10.1097/00000658-199101000-00005.

125. Schneider, K., Nelson, G.M., Watson, J.L., Morf, J., Dalglish, M., Luh, L.M., Weber, A., and Bertolotti, A. (2020). Protein Stability Buffers the Cost of Translation Attenuation following eIF2α Phosphorylation. Cell Rep. *32*, 108154. https://doi.org/10.1016/j.celrep.2020.108154.

126. Adams, C.M. (2007). Role of the transcription factor ATF4 in the anabolic actions of insulin and the anti-anabolic actions of glucocorticoids. J. Biol. Chem. *282*, 16744–16753. https://doi.org/10.1074/jbc.M610510200.

127. Byles, V., Cormerais, Y., Kalafut, K., Barrera, V., Hughes Hallett, J.E., Sui, S.H., Asara, J.M., Adams, C.M., Hoxhaj, G., Ben-Sahra, I., and Manning, B.D. (2021). Hepatic mTORC1 signaling activates ATF4 as part of its metabolic response to feeding and insulin. Mol. Metabol. *53*, 101309. https://doi.org/10.1016/j.molmet.2021.101309.

128. Kilkenny, C., Browne, W.J., Cuthill, I.C., Emerson, M., and Altman, D.G. (2010). Improving bioscience research reporting: the ARRIVE guidelines for reporting animal research. PLoS Biol. *8*, e1000412. https://doi.org/10.1371/journal.pbio.1000412.

STAR★METHODS

KEY RESOURCES TABLE

REAGENT or RESOURCE	SOURCE	IDENTIFIER
Antibodies		
Rabbit monoclonal anti-phospho-(S51)-eIF2α	Abcam	Cat#ab32157; RRID: AB_732117
Rabbit polyclonal anti-eIF2α	Cell Signaling Technology	Cat#9722; RRID: AB_2230924
Rabbit polyclonal anti-phospho-(S240/244)-rpS6	Cell Signaling Technology	Cat#2215; RRID: AB_331682
Rabbit monoclonal anti-rpS6	Cell Signaling Technology	Cat#2217; RRID: AB_331355
Goat polyclonal anti-phospho-[Y705]-STAT3	Santa Cruz Biotechnology	Cat#sc-7993; RRID: AB_656682
Rabbit monoclonal anti-STAT3	Cell Signaling Technology	Cat#4904; RRID: AB_33126
Rabbit polyclonal anti-phospho-[S757]-ULK1	Cell Signaling Technology	Cat#6888; RRID: AB_10829226
Rabbit polyclonal anti-ULK1	Sigma-Aldrich	Cat#A7481; RRID: AB_1840703
Rabbit polyclonal anti-LC3B	Novus Biotechnology	Cat#NB100-2220; RRID: AB_10003146
Goat anti-rabbit	Cell Signaling Technology	Cat#7074; RRID: AB_2099233
Horse anti-mouse	Cell Signaling Technology	Cat#7076; RRID: AB_330924
Chemicals, peptides, and recombinant proteins		
Amino acid mixture-^{13}C,^{15}N	Sigma-Aldrich	Cat#487910
TGX Stain-Free™ FastCast™ Acrylamide Kit, 10%	Bio-Rad Laboratories	Cat#1610183
Critical commercial assays		
ELISA Kit for mouse IL-6	R&D Systems	Cat#M6000B; RRID: AB_2877063
ELISA Kit for mouse GDF15	R&D Systems	Cat#DY6385; RRID: AB_3083003
ELISA Kit for mouse SAA	Tridelta Development Ltd	Cat#TP 802M
AccQ-Tag Ultra Derivatization Kit	Waters	Cat#186003836
Nucleospin RNA Kit	Macherey Nagel	Cat#740955
ddPCR Evagreen SuperMix	Bio-Rad Laboratories	Cat#186-4035
SSO Advanced Universal SYBR Green Supermix	Bio-Rad Laboratories	Cat#1725274
Experimental models: Cell lines		
C26 murine colon adenocarcinoma cells	Pr. Laure Bindels laboratory	N/A
Experimental models: Organisms/strains		
Mouse: CD2F1 male mice	Charles River Laboratories	Cat#033CDF-1; RRID:IMSR_CRL:033
Oligonucleotides		
See Table S1 for qPCR primers	Sigma-Aldrich Genosys	N/A
Software and algorithms		
ImageJ v1.54	ImageJ	https://imagej.net/ij/; RRID:SCR_003070
Prism 9.0	GraphPad	https://www.graphpad.com/; RRID:SCR_002798
QX Manager, Standard Edition, v 1.2.345	Bio-Rad Laboratories	https://www.bio-rad.com/fr-fr/life-science/digital-pcr/qx-software

EXPERIMENTAL MODEL AND STUDY PARTICIPANT DETAILS

All mandatory laboratory health and safety procedures have been complied with in the course of conducting any experimental work reported in this paper.

Cell culture

C26 is a murine colon adenocarcinoma that was initially induced by N-nitroso-N-methylure, known to induce cachexia in syngeneic hosts.[38] C26 cells (provided by Pr. L. B. Bindels) were maintained in high-glucose Dulbecco's modified Eagle's medium, supplemented with 10% fetal bovine serum and 100 units/ml penicillin and streptomycin, at 37°C with 5% CO2.

Animal experiments

All animal experiments were carried out in accordance with the guidelines of the local ethics committee (CEEA-02), as well as French and European Union laws: permission to experiment on mice APAFIS#24596–2020012713544797 v5 and animal facilities agreement E6334515. To describe animal experiments, we have taken into account the recommendations of the ARRIVE Guidelines for Reporting Animal Research.[128] We used the C26 mouse model of cancer cachexia, which is associated with both anorexia, body weight reduction and loss of muscle mass.[19,55] Eight-week-old CD2F1 male mice were purchased from Charles River Laboratories, France. They were housed individually in the presence of an environmental enrichment element (a plastic tube-shaped cache), at an ambient temperature of 22°C and according to a standard 12h/12h light/dark cycle. Throughout the experiment, mice had free access to standard food (Safe Cat# A03, 52% carbohydrate, 5.1% lipids, and 21.4% proteins) and tap water. After sixteen days of acclimatization, animals were assigned to the different groups so as to obtain a homogeneous distribution of animals according to body weight. The average body weight was 24.9 g at the time of intervention. Mice were inoculated subcutaneously and intra-scapularly with 10^6 C26 cells in 0.15 mL of NaCl 9/1000 (n = 13). Control mice were injected with 0.15 mL of NaCl 9/1000 (sham-injected mice; n = 9). These procedures were performed in the same session for all mice. Food intake and body weight were measured every 24 h (this measurement was always performed at the same time at the end of the dark period). Food consumption was monitored using specific cages developed by our team, equipped with removable external feeders including crumb collectors, allowing precise measurement of food intake. Time points of sacrifice by necropsy were determined accordingly to our objective to analyze and compare two stages: before the onset of cachexia (pre-Cx) on day 6 post-implantation of C26 cells and at the onset of cachexia (Cx) on day 8. The sham-injected group combined control mice on days 6, 7 and 8 post-injection of NaCl (we observed no significant variation between samples taken on different days for any of the parameters analyzed in the sham-injected group). Sacrifices were performed 5–6 h after the beginning of the light period. Blood was collected by cardiac puncture under deep general anesthesia of the animals with isoflurane, then treated with EDTA. Plasma samples were obtained by centrifugation and stored at −80°C until use. The animals were then subjected to death by cervical dislocation before tumors, tissues and organs were harvested, weighed and frozen on dry ice and stored at −80°C until processing.

METHOD DETAILS

RNA extraction & cDNA synthesis

Tissues were powdered on dry ice (except hypothalamus), then crushed using a vibrating shredder (Retsch MM 400) in the first extraction step. Total RNA was isolated using Nucleospin RNA Kit from Macherey Nagel (Cat#740955) and treated with DNase I, Amp Grade (Invitrogen, Cat#18068015) prior to cDNA synthesis. After RNA extraction, RNA concentration was measured using a NanoDrop One (ThermoFisher Scientific). RNA (0.5 μg) was reverse transcribed with 100 U of Superscript II Reverse Transcriptase (Invitrogen, Cat#18064014) using 100 μM random hexamer primers (Invitrogen, Cat#48190011), according to the manufacturer's instructions.

Digital qPCR

Droplet digital PCR (ddPCR) was performed using a QX200 Droplet Digital PCR system (Bio-Rad Laboratories). The ddPCR reactions were carried out into a final volume of 20 μL comprising 10 μL of 2X QX200 ddPCR Evagreen SuperMix (Bio-Rad Laboratories, Cat#186–4035), 0.1 μM each of forward and reverse primers, and 5 μL cDNA. For primer sequences, see Table S1. Droplets were generated in eight-well cartridges using the QX200 droplet generator (Bio-Rad Laboratories) prior to PCR amplification on the C1000 Thermal Cycler (Bio-Rad Laboratories). The PCR parameters were as follows: initial denaturation/activation step at 95°C for 10 min then 50 cycles of 30 s denaturation at 95°C, and annealing/extension at 57°C for 1 min followed by 98°C for 10 min and a final hold at 4°C. After PCR the droplets were individually analyzed using the QX200 droplet reader (Bio-Rad Laboratories) and data were processed with QX Manager Software, Standard Edition, v 1.2.345. Only reactions generating more than 10,000 droplets were considered valid.

Conventional qPCR

Real-time quantitative PCR was performed on a Bio-Rad CFX-96 detection system with quantitative PCR SSO Advanced Universal SYBR Green Supermix (Bio-Rad Laboratories, Cat#1725274) and with a primer concentration of 0.5 μM. PCR conditions were standardized to 40 cycles of 95°C for 10 s and 59°C for 30 s with the primers (Sigma-Aldrich Genosys) for specific mouse mRNA sequences. For primer sequences, see Table S1. Quantification of mRNA expression was performed according to the delta-delta Ct method.

Protein extraction

Tissues were powdered on dry ice, then crushed using a vibrating shredder (Retsch MM 400) in the first extraction step. Total proteins were extracted from liver samples with 1X Laemmli buffer, as previously described.[37] Protein extracts were prepared from spleen tissue using RIPA buffer as previously described.[127] Protein samples were boiled at 95°C for 10 min before electrophoresis.

Western-blot analysis

Proteins were resolved by SDS-PAGE on 10% TGX-polyacrylamide gels (TGX Stain-FreeFastCast Acrylamide Kit, Bio-Rad Laboratories Cat#1610183) in Tris-glycine-SDS buffer. Protein transfer was performed at 4°C in Tris-glycine buffer onto polyvinylidene

fluoride (PVDF) membranes (Amersham Hybond P0.45, Cat# 10600023). We used the TGX system for non-specific detection of all proteins. This signal was acquired both on electrophoresis gels after migration (not shown) in order to check the quantity of loaded proteins, but also on PVDF membranes just after transfer for controlling its efficiency. Membranes were blocked with non-fat dried milk powder (5% w/v) diluted in TBS-Tween for 1 h, then incubated with primary antibodies diluted in TBS-Tween containing 5% BSA (dilution according to manufacturer's instructions) overnight at 4°C, then washed 3 times for 5 min in TBS-Tween. HRP-coupled anti-species secondary antibodies were diluted at 1:2000 in TBS-Tween containing 5% (w/v) non-fat dried milk and used at room temperature for 1 h. Membranes were washed 3 times for 5 min in TBS-Tween, then rinsed in TBS before analysis. Luminata western HRP substrate (Millipore, WBLUR0500) and a chemi-luminescence imager (G:box, Syngene) were used to detect signals. Signal intensities were quantified using the ImageJ software (RRID: SCR_003070). For a given sample, the respective intensities of LC3-I and LC3-II signals were quantified from the same selected area. Relative quantifications have been performed, with mean control condition value normalized to 1.

Antibodies

Anti-phospho-(S51)-eIF2α antibody was from Abcam (Cat#ab32157; RRID: AB_732117) and anti-phospho-[Y705]-STAT3 antibody from Santa Cruz Biotechnology (Cat#sc-7993; RRID: AB_656682). Antibodies targeting eIF2α (Cat#9722; RRID: AB_2230924), phospho-[S757]-ULK1 (Cat#6888; RRID: AB_10829226), phospho-(S240/244)-rpS6 (Cat#2215; RRID: AB_331682), rpS6 (Cat#2217; RRID: AB_331355) and STAT3 (Cat#4904; RRID: AB_331269) were from Cell Signaling Technology, as well as anti-species secondary antibodies coupled to horseradish peroxidase: anti-rabbit antibody (Cat#7074; RRID: AB_2099233) and anti-mouse antibody (Cat#7076; RRID: AB_330924). Anti-LC3B antibody was purchased from Novus Biotechnology (Cat#NB100-2220; RRID: AB_10003146) and anti-ULK1 from Sigma-Aldrich (Cat#A7481; RRID: AB_1840703).

ELISA

IL-6, GDF15 and SAA were detected in EDTA-treated plasma samples using commercially available ELISA kits (R&D Systems, Cat#M6000B, RRID: AB_2877063 for mouse IL-6; R&D Systems, Cat#DY6385, RRID: AB_3083003 for mouse GDF15; Tridelta Development Ltd, Cat#TP 802M, for mouse SAA), according to the manufacturer's instructions.

Plasma amino acid analysis

For sample preparation, 25 μL of plasma were vortexed with 25 μL of the internal standard solution (mixture of labeled AA isotopes; Sigma-Aldrich, Cat#487910) and 150 μL of methanol with 0.1% formic acid at −20°C. The extract was left at −20°C during 30 min to precipitate the proteins then centrifuged at 14000 rpm for 10 min. After that, for derivatization reaction, 10 μL of the supernatant was mixed with 70 μL of borate buffer (pH 8.8) and 20 μL of the AQC solution (AccQ·Tag Ultra Derivatization Kit, Waters, Cat#186003836) and the reaction mixtures were heated at 55°C for 10 min before LC/MS analysis. A standard mixture solution contained 100 mg/L of each amino acid was prepared in water then calibration solutions were realized by dilution in water at concentrations between 0.1 and 100 mg/L. Before LC/MS analysis, 25 μL of each calibration solution was taken to derivatization reaction with the same method as plasma sample. Chromatographic separation was performed with an Ultimate 3000 UHPLC (Thermo Scientific) and a CORTECS C18 (150 mm × 2.1 mm; 1.6μm) column (Phenomenex) maintained at 55°C. The mobile phases consisted of water (A) and acetonitrile (B), both with 0.1% formic acid. The LC gradient used was as follows: from 99% A hold for 1 min, then to 87% A in 1 min, then to 85% A in 3.5 min; then to 5% A in 1 min finally 5% A was maintained 1 min and went back to the initial conditions within 0.1 min for an equilibration time of 1.4 min. The flow rate was 0.5 mL/min and the injection volume was 5 μL. The detection was performed with a Q Exactive mass spectrometer (Thermo Scientific) using positive electrospray ionizations, in SRM mode. The desolvation temperature was 438°C and capillary temperature was 320°C. The gas (N_2) flow rates (arbitrary unit) were set at 53 for Sheath gas, 14 for Aux gas and 3 for Sweep gas. The spray voltage was 3.5 kV with an S Lens level RF Level at 60. The mass resolution was set at 35000, automatic gain control at 10^6 and injection time at 50 ms.

QUANTIFICATION AND STATISTICAL ANALYSIS

Groups were composed of $N = 9$ NaCl-injected mice for the Sham group, $N = 7$ C26-injected mice for the Pre-Cx group and $N = 6$ C26-injected mice for the Pre-Cx group. No mice were excluded from the study. Data are presented as mean ± standard error of the mean (SEM). To evaluate the significance of the difference of both food intake and body weight between groups over time, two-way analyses of variance (Anova) were performed for each of these parameters and completed by Tukey's multiple comparison tests to analyze differences between groups at each time point (see the legend of Figure 1). For other analyses, one-way Anova followed by Tukey's multiple comparisons were performed to compare and assess the significance of differences between the three groups with each other. Statistical analyses were performed using GraphPad Prism 9.0 (RRID:SCR_002798). $p < 0.05$ was considered statistically significant (*$p < 0.05$; **$p < 0.01$; ***$p < 0.001$; ****$p < 0.0001$). In some cases, *t*-tests were performed to assess the significance of differences by pairwise comparison between two specific groups (mentioned in the text; #$p < 0.05$ by t-test).